Alma Mater Studiorum – University of Bologna

SCHOOL OF SCIENCE
Department of Industrial Chemistry "Toso Montanari"

Second cycle degree in

Low Carbon Technologies and Sustainable Chemistry

Classe LM-71 - Scienze e Tecnologie della Chimica Industriale

Synthesis and Characterization of Iron Carbide Carbonyl Clusters

Experimental degree thesis

CANDIDATE

Gian Luca Manfredini

SUPERVISOR

Chiar.mo Prof. Stefano Zacchini

CO-SUPERVISOR

Dott.ssa Cristiana Cesari

Dott.ssa Francesca Forti

Academic Year 2021-2022

ABSTRACT

This study is focused on the synthesis, characterization and reactivity of new low nuclearity iron carbide carbonyl clusters. In particular, the oxidation of the highly reduced monocarbide tetraanionic cluster $[Fe_6C(CO)_{15}]^{4-}$ was studied in details using different oxidants ($[Cp_2Fe][PF_6]$, $HBF_4{\cdot}Et_2O$, MeI and EtI), different stoichiometries and experimental conditions. Different products were obtained depending on the reaction conditions, among which previously reported $[Fe_6C(CO)_{16}]^{2-}$ and $[Fe_5C(CO)_{14}]^{2-}$, and new $[Fe_6C(CO)_{14}(CO)_{13}]^{4-}$ and $[Fe_5C(CO)_{13}(COMe)]^{3-}$ were isolated and fully characterized.

In the second part of this study, the reactions of $[Fe_6C(CO)_{15}]^{4-}$ with organic or inorganic molecules containing sulphur (S_8, S_2Cl_2 and PhSH) were investigated aiming at introducing S-atoms within the structure of iron carbide carbonyl clusters. In particular, the reaction of $[Fe_6C(CO)_{15}]^{4-}$ with PhSH afforded the new $[Fe_6C(CO)_{14}(SPh)]^{3-}$ cluster. Conversely, using S_8 and S_2Cl_2, oxidation of $[Fe_6C(CO)_{15}]^{4-}$ occurred following a path similar to that observed with other oxidizing agents.

All these species have been analyzed by Single Crystal X-ray diffraction (SC-XRD) and IR spectroscopy.

INDEX

1. Introduction *1*

1.1 Metal carbonyl clusters **1**

1.2 Metal Carbide Carbonyl Clusters **6**

2. Results and Discussions *12*

2.1 Synthesis of $[Fe_6C(CO)_{15}]^{4-}$ **12**

2.2 Oxidation of $[Fe_6C(CO)_{15}]^{4-}$: General features **15**

2.3 Reactions of $[Fe_6C(CO)_{15}]^{4-}$ with MeI **21**

2.4 Reactions of $[Fe_6C(CO)_{15}]^{4-}$ with S-based reagents **27**

3. Conclusions *31*

4. Experimental part *32*

4.1 General Procedures **32**

4.2 Synthesis of $[NEt_4]_4[Fe_6C(CO)_{15}]$ **32**

4.3 Reaction of $[NEt_4]_4[Fe_6C(CO)_{15}]$ with MeI in the presence of Na_2CO_3: Synthesis of $[NEt_4]_3[Fe_5C(CO)_{13}(COMe)]$ **33**

4.4 Reaction of $[NEt_4]_4[Fe_6C(CO)_{15}]$ with MeI: Synthesis of $[NEt_4]_3[Fe_5C(CO)_{13}(COMe)]$ **34**

4.5 Reaction of $[NEt_4]_4[Fe_6C(CO)_{15}]$ with EtI in the presence of Na_2CO_3: Synthesis of $[NEt_4]_3[Fe_5C(CO)_{13}(COEt)]$ **35**

4.6 Reaction of $[NEt_4]_4[Fe_6C(CO)_{15}]$ with EtI: Synthesis of $[NEt_4]_3[Fe_5C(CO)_{13}(COEt)]$ and $[NEt_4]_3[H_3O][Fe_6C(CO)_{14}(CO_3)]$ **36**

4.7 Reaction of $[NEt_4]_4[Fe_6C(CO)_{15}]$ with $HBF_4 \cdot Et_2O$: Synthesis of $[NEt_4]_2[Fe_5C(CO)_{14}]$ **37**

4.8 Reaction of $[NEt_4]_4[Fe_6C(CO)_{15}]$ with $[Cp_2Fe][PF_6]$ **38**

4.9 Reaction of $[NEt_4]_4[Fe_6C(CO)_{15}]$ with S_8 ..... **39**

4.10 Reaction of $[NEt_4]_4[Fe_6C(CO)_{15}]$ with PhSH: Synthesis of $[NEt_4]_3[Fe_6C(CO)_{14}(SPh)]$ **39**

4.11 Reaction of $[NEt_4]_4[Fe_6C(CO)_{15}]$ with S_2Cl_2 ..... **41**

5. References *43*

1. Introduction

1.1 Metal carbonyl clusters

The term "Metal Cluster" was introduced in 1966 by Frank Albert Cotton to describe a class of compounds "*containing a finite group of metal atoms which are held together entirely, mainly, or at least to a significant extent, by bonds directly between the metal atoms even though some non-metal atoms may be associated intimately with the cluster*". [1]

The huge interest regarding this class of compounds is mainly given by the fact that they possess intermediate properties between those of bulk metals and single metal ions.

Due to these properties, metal clusters are situated in the area comprised between molecular compounds, metallic nanoparticles and colloids (**Figure 1.1**).

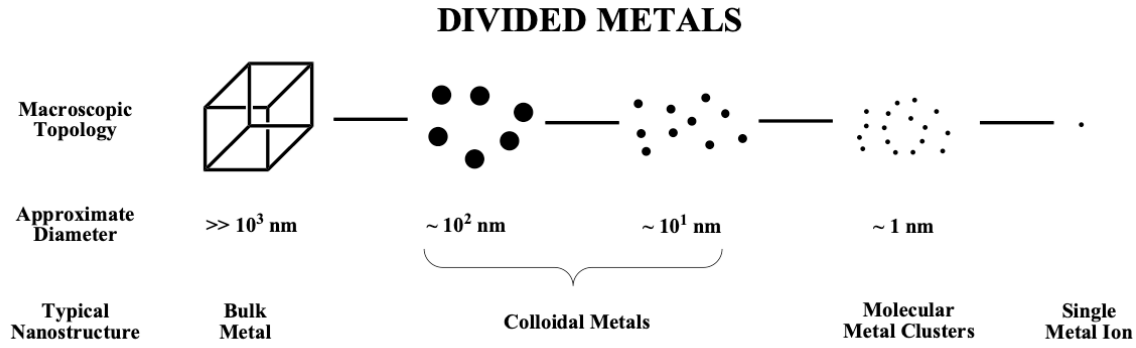

Figure 1.1 – Representation of the size of bulk metal, colloidal metals, metal clusters and single metal ions.

Metal clusters are usually stabilized by the coordination on their surfaces of ligands, such as CO, halides, hydrides, phosphines, thiols. Analyzing the different ligands, one molecule that has the most stabilizing power in this field is carbon monoxide (CO) because it has the peculiarity to bind to metals through σ donation as well as π back-donation.[2] Indeed, it can donate a couple of electrons to the empty orbitals of the metal acting as Lewis base (σ donation). At the same time, CO can accept electrons from the metal on its empty π* orbitals acting as Lewis acid (π back-donation).

The synergy between σ donation and π back-donation makes CO a very strong ligand, also justifying its position at the end of the spectrochemical series.

Another important thing that need to be outlined is the fact that CO displays limited steric dimensions; this is an important point because through this fundamental property no issues were registered regarding the steric hindrance. Moreover, CO can bind to metals as terminal ligand, as well as edge bridging and face capping ligand.

Taking into consideration the number of ligand molecules bonded to a metal cluster, this depends on some electron-counting rules, even if exceptions are known, which become very common in the case of large clusters.[3,4] The valence electrons of a cluster result from the addition of the valence electrons of the metals, those donated by the ligands and the overall negative charge. In general, a certain number of Cluster Valence Electrons (CVE) is required to fill all the Valence Molecular Orbitals (CVMO) of the cluster itself.

The routes of interest through which metal clusters can obtained are mainly four: [5]

a) Direct or Reductive Carbonylation

On one hand, direct carbonylation consists in the reaction between the powder of the metal and carbon monoxide; this reaction can be carried out in a quite good manner only with Ni and Fe.

On the other hand, metal carbonyls can be obtained starting from the salt of the metal of interest, under atmosphere of CO and in the presence of a reducing agent. CO itself can be used in some cases as reducing agent, and the capacity of CO to act as a reducing agent is enhanced in the presence of bases, as depicted in **equation 1.1**.

$$CO + 2OH^- \longrightarrow CO_2 + H_2O + 2e^- \qquad (1.1)$$

b) Thermal Methods

Thermal methods are based on the elimination of one or more CO ligand and this is an endothermic process. When CO ligands are eliminated from the clusters, different effects can be seen, such as: stabilization of the cluster itself due to the loss of CO groups, permutation of the metallic atoms present in the structure and intra/intermolecular condensation.

c) Redox Methods

The first studies made on redox methods were carried out by Hieber [6] on carbonyl clusters of Iron. These methods were further investigated and extended to other metals by Paolo Chini. [7]

Redox methods are useful because through them it is possible achieving the synthesis of compounds at low or high nuclearity. The reductions can be done in two different ways: the first one is with the direct addition of electrons coming from alkaline metals present in solution; instead, the second method is mainly based through the nucleophilic attack of OH^- ions to the carbon of a coordinated carbonyl group.

In both cases, the main thing which is observable is the fact that the reduced metal can be sufficiently stable to remain as fragment coming from the initial compound, or it can undergo redox condensation in order to increase the nuclearity of the cluster, as shown in **Scheme 1.1**.

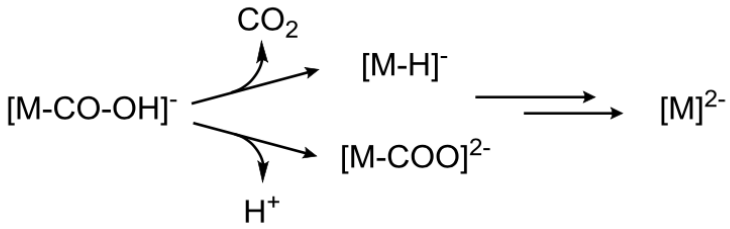

Scheme 1.1 - Reduction of a metal through the addition of OH^-.

The oxidation of a cluster is carried out with non-coordinating reagents, such as the Ferrocenium ion treated in my thesis, in which the main evidence is the formation of new M-M bonds even if there is the possibility in having no loss of CO groups in the structure.

The reaction of metal carbonyls with salts or metallic complexes, leads also to the formation of bimetallic clusters through redox condensation.

d) Chemically induced methods

Preformed metal carbonyl clusters can be modified in different ways in order to allow the formation of new species. These new clusters can be formed through the addition of nucleophiles, which leads to two different results: 1) removal of ML_x fragments degrading the clusters at high nuclearity to smaller species; 2) condensation with formation of clusters at higher nuclearity.

Generally talking about metal carbonyl clusters (MCC), a distinction between clusters with high and low nuclearity needs to be done. The nuclearity of a cluster is given by the total number of metal atoms. Another important parameter is the CO/M ratio.

This ratio decreases as the nuclearity increases. At the same time, also the number of M-M bonds increases with increasing nuclearity. Thus M-M bonds become more important than M-CO bonds as the nuclearity of the cluster increases. The increase of M-M bonds leads also to metallization of the metallic core of the cluster.

Considering the molecular orbitals, what happens during the metallization is the transition from a small molecule in which all the electrons are localized in a quite good way to a large cluster characterized by an electronic system strongly delocalized.[5]

The HOMO-LUMO gap is usually big in a system in which the nuclearity is low; then, as the nuclearity of the cluster (and the number of M-M bonds) increases, the HOMO-LUMO gap decreases.

All these assumptions give us a proper background to understand the chemistry of clusters; thinking about MCCs at low nuclearity, these will follow the 18 electron rule.

This means that each metal atom, which is able in composing the nucleus of the cluster, tends to reach the complete occupation of 9 valence molecular orbitals (6 bonding and 3 non-binding) as shown in the **Figure 1.2**.

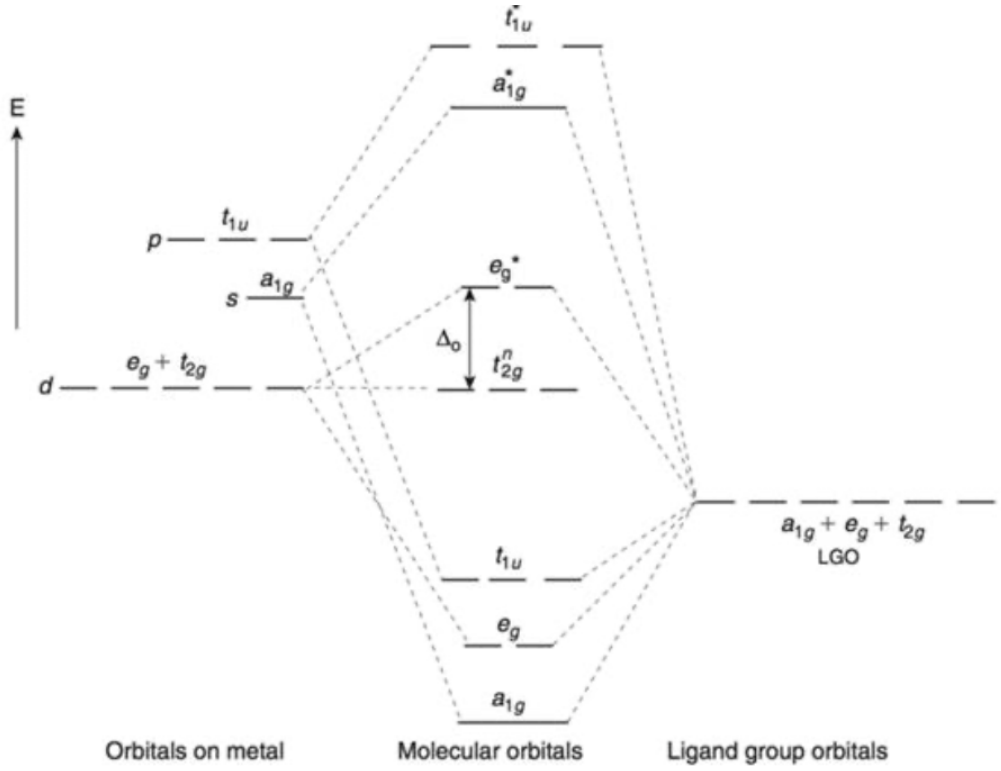

Figure 1.2 – Simplified representation of the MO diagram of a coordination compound.

When the bond between the metal and CO groups is present, the main advantage coming from it is the stabilization of the low oxidation state through the π back donation.

The ligands present in clusters are mainly π acceptors. The σ-donation / π back donation mechanism allows the redistribution of the electronic density from the metal to the CO. This characteristic is important because the whole system tends to an electroneutral state, which promotes a greater stability.

Considering the CO group, the orbitals involved in π back donation are the anti-bonding π* LUMO of the C≡O bond.

MCCs in that way are stabilized thanks to a system which is characterized by two peculiarities: σ donation of electrons coming from the HOMO of the carbonyl group to the metal and back donation from the metal to the CO, with a consequent formation of the π bond, as shown in **Figure 1.3**.

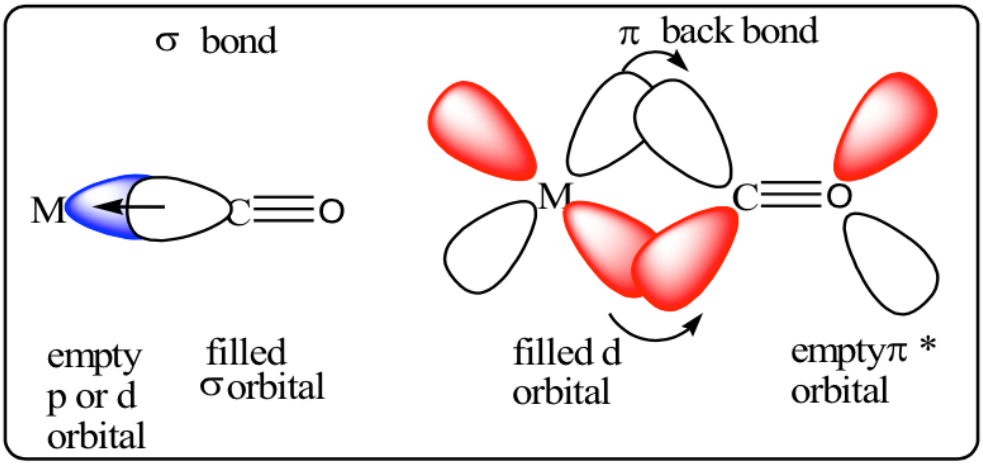

Figure 1.3 – Representation of the M-CO bond with back donation.

Regarding the phenomenon just described, from an experimental point of view it has some consequences which are fundamental in order to characterize all the compounds; in particular, when the anti-bonding orbital of the carbonyl group is populated the strength of the bond between C and O is diminished.

This is mainly observable through IR spectroscopy because the stretching frequencies of the carbonyl group move from a value of 2143 cm^{-1} as pure triple bond in free CO gas, to 2125-1850 cm^{-1} in M-CO compounds containing only terminal carbonyls, and eventually to 1850-1700 cm^{-1} in the presence of edge bridging or face capping CO ligands.

1.2 Metal Carbide Carbonyl Clusters

The square pyramidal $Fe_5C(CO)_{15}$ species was the first structurally characterized metal carbonyl cluster (MCC) containing a semi-exposed C-atom.[8] Soon after, the structure of the octahedral $Ru_6C(CO)_{17}$ cluster was unravelled by single crystal X-ray diffraction (SC-XRD), showing the presence of a fully interstitial carbide atom.[9] Several other metal carbide carbonyl clusters were, then, discovered including species containing interstitial or semi-interstitial (semi-exposed) C-atoms, as well as species containing one or more carbide atom.[10-12]

Clusters containing semi-exposed carbide atoms are interesting because of the reactivity of the semi-exposed C-atom,[13-16] which represents an useful model for relevant industrial processes, such as the Fischer-Tropsch reaction.[17-20]

From the other side, fully interstitial carbide atoms are not accessible to reagents, and display a limited (or almost null) direct reactivity. Nonetheless, they play a fundamental role in the stabilisation of metal carbonyl clusters in two synergic ways: [21,22]

a) Formation of additional M-C bonds, which add to M-M bonds, reinforcing the metal cage of the cluster. This issue is very important for first raw transition metals such as Fe, Co and Ni, because the strength of their M-M bonds is really weak.

b) Interstitial carbides act also as internal ligands lowering the number of CO groups present in the surface of the clusters and limiting steric problems. In order to explain this point, it is necessary to consider two elements and make a comparison between them; these are Ru and Fe. Ruthenium forms both clusters without the presence of carbides such as $[Ru_6(CO)_{18}]^{2-}$, or with the presence of carbides like $[Ru_6C(CO)_{16}]^{2-}$.[23] Conversely, making a comparison with Fe, the only compound which is known is $[Fe_6C(CO)_{16}]^{2-}$ [24] in which the carbide is present. This is mainly because Fe is smaller than Ru, and in the surface of a Fe_6 octahedron there is not enough space for 18 CO ligands.

The stability given by these two synergic effects results in the fact that all the clusters which are characterized by the presence of an interstitial carbide in their structure can reach higher nuclearities with respect to those that are constituted only by CO ligands.

In addition, the enhanced stability conferred by the carbide atoms allows for a variety of chemical and electrochemical reactions on the surface of the cluster.[25]

MCCs nowadays have attracted the interest due to different factors. First of all, the discovery of the presence of a Fe-S-carbide cluster in the active site of the nitrogenase enzymes [26-28] stimulated a great interest in studying Fe carbide carbonyl clusters and the possibility to insert S-atoms into their structures. [29-33]

Moreover, Fe and Co carbide carbonyl clusters have shown high performances as electrocatalysts for the hydrogen evolution reaction (HER). [34-36] In addition to that, MCCs with an high nuclearity, including also large carbide carbonyl clusters and nanoclusters, were considered useful also in making a contribution to nanochemistry. [5,12,25,37]

Metal carbide carbonyl clusters can be directly obtained through three general synthetic procedures: [5,12,21,38]

1) Thermal disproportionation of CO to C and CO_2, upon heating of simple metal carbonyls. This has been widely used in the case of Re, Fe, Ru and Os carbonyls.

2) CO splitting given by the reduction of a bridging CO ligand. This process occurs through the coordination of a Lewis acid (e.g., RCO^+, generated from RCOCl) to the O atom of a bridging carbonyl resulting in the formation of $[M_n]$-C-O-C(O)R species. After that, the reduction of this species is performed, resulting in a metal carbide with the consequent elimination of $RCOO^-$. This approach is useful for synthesis of some Fe and Co carbide carbonyl clusters.

3) Direct reaction of a metal carbonyl anion with carbon halides (CCl_4, C_2Cl_4, C_2Cl_6, C_3Cl_6). This procedure has been largely employed for the synthesis of Co, Rh, and Ni carbide carbonyl clusters.

Once prepared, carbide carbonyl clusters can be used as starting materials in different types of reactions, such as thermal reactions, oxidations, reduction, redox condensation, reactions with Lewis acids and with nucleophiles. All of them can modify the staring carbide carbonyl clusters transforming them into new species. [5,12,21,22]

1.3 Iron Carbide Carbonyl Clusters

Based on their structures, Homometallic Iron Carbide Carbonyl Clusters can be classified into three different categories:

1. Fe_4C clusters with a butterfly structure, which display a semi-exposed carbide, such as $[Fe_4C(CO)_{13}]$ and $[Fe_4C(CO)_{12}]^{2-}$. [39]

2. Fe_5C clusters with a square pyramidal structure, which possesses a basal semi-exposed carbide, such as $[Fe_5C(CO)_{15}]$ and $[Fe_5C(CO)_{14}]^{2-}$.[40]

3. Fe_6C octahedral clusters incorporating a full interstitial carbide atom, such as $[Fe_6C(CO)_{16}]^{2-}$ and $[Fe_6C(CO)_{15}]^{4-}$.[41]

Some of these Iron Carbide Carbonyl Clusters can be directly accessed by thermal disproportionation of CO ligands (**Scheme 1.2**). For instance, heating iron pentacarbonyl, $Fe(CO)_5$, in the presence of quinoline results in the formation of $[Fe_6C(CO)_{16}]^{2-}$.

This species can be further modified affording new Fe carbide carbonyl clusters. As an example, the highly reduced species $[Fe_6C(CO)_{15}]^{4-}$ can be obtained by reduction of $[Fe_6C(CO)_{16}]^{2-}$ with NaOH in DMSO.[41] This reaction will be explained in details in **Paragraph 2.1** being $[Fe_6C(CO)_{15}]^{4-}$ the staring material employed in this Thesis.

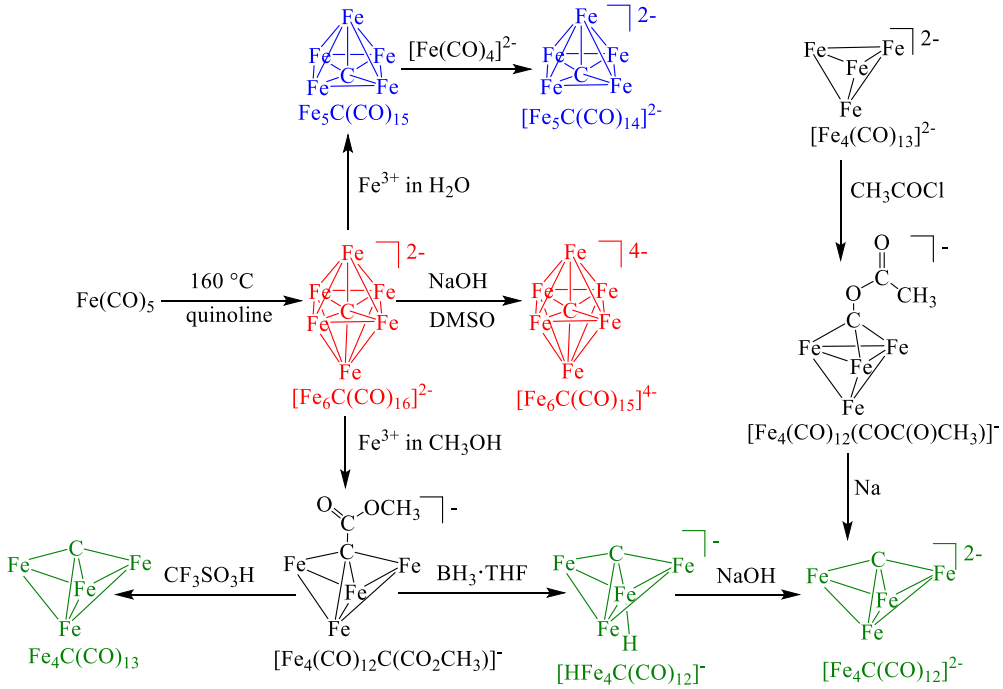

Scheme 1.2 - Synthesis of Fe carbide carbonyl clusters. All the species have been isolated and fully characterized in literature. $[Fe_6C(CO)_{16}]^{2-}$ is prepared directly from $Fe(CO)_5$ by thermal treatment. Other Fe carbide carbonyl clusters can be obtained from $[Fe_6C(CO)_{16}]^{2-}$ using redox reactions. Alternatively, $[Fe_4C(CO)_{12}]^{2-}$ can be prepared starting from $[Fe_4(CO)_{13}]^{2-}$ in a two-step reaction by CO scission. CO ligands have been omitted for clarity.

Iron carbide carbonyl cluster, from an historical point of view, are important. The square pyramidal $Fe_5C(CO)_{15}$ was the first metal carbonyl cluster containing a carbide atom which was analyzed and then, structurally characterized.[8]

All the studies about the structures and the reactivity of Fe carbide carbonyl clusters largely contribute to the development of the cluster-surface analogy and Fisher-Tropsch chemistry. [13-20]

Fe-C-CO clusters undergo some common reactions such as reduction, oxidation, fragmentation, protonation, hydrogenation and alkylation. These different reactions, in some cases, lead to the formation of new C-H and C-C bonds.

Looking at all the clusters listed until now, one of the main interesting things regards the cluster constituted by Fe and S since an Iron-Sulfide carbide cluster was found in the active site of FeMoCo [26-28] cofactor of nitrogenase and the so called 'carbide problem' became a paramount of importance in bioinorganic chemistry.

Some possible approach for the preparation of Fe-S-carbide clusters involve the use of $[Fe_6C(CO)_{16}]^{2-}$ as starting material. [29-33]

The octahedral cluster, $[Fe_6C(CO)_{14}(S)]^{2-}$, containing one carbide and one sulfide can be obtained in a multistep synthesis (**Scheme 1.3**): 1) substitution of one CO ligand of $[Fe_6C(CO)_{16}]^{2-}$ with SO_2 to form $[Fe_6C(CO)_{15}(SO_2)]^{2-}$; 2) methylation of the latter with CF_3SO_3Me to give $[Fe_6C(CO)_{15}(SO_2Me)]^{-}$; 3) reduction to $[Fe_6C(CO)_{14}(S)]^{2-}$.

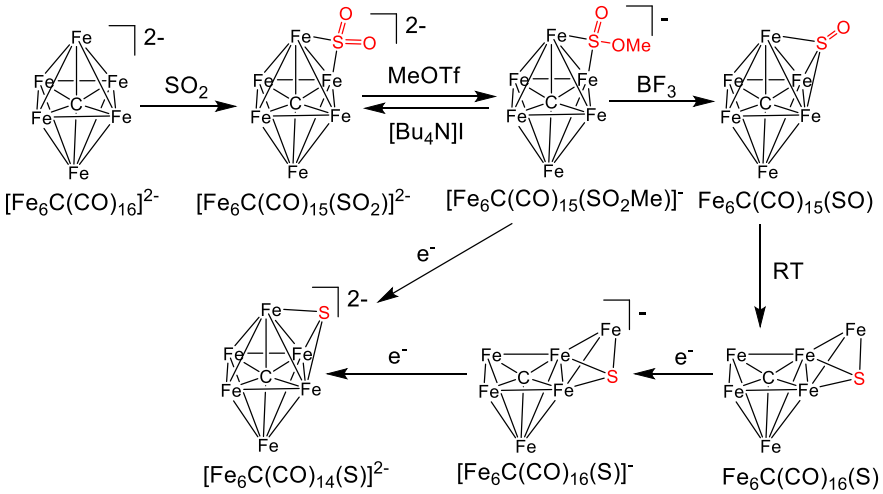

Scheme 1.3 - Synthesis of $Fe_6C(CO)_{16}(S)$ and $[Fe_6C(CO)_{14}(S)]^{2-}$. $[Fe_6C(CO)_{16}]^{2-}$ is transformed into $[Fe_6C(CO)_{15}(SO_2)]^{2-}$ by CO substitution with SO_2. Further reactions with MeOTf, BF_3 and reduction with Na/naphthalene result in the target compounds. CO ligands have been omitted for clarity.

Alternatively, the direct reaction of $[Fe_6C(CO)_{16}]^{2-}$ with S_2Cl_2 or S_8 affords mixtures of clusters, among which the μ_4-S^{2-} bridged μ_5,μ_6-bis(carbide) cluster $[\{Fe_5(\mu_5\text{-}C)(CO)_{13}\}\{Fe_6(\mu_6\text{-}C)(CO)_{15}\}(\mu_4\text{-}S)]^{2-}$ (a) and the symmetric μ_4-S^{2-} bridged μ_5,μ_5-bis(carbide) cluster $[\{Fe_5(\mu_5\text{-}C)(CO)_{13}\}_2(\mu_4\text{-}S)]^{2-}$ (b) have been isolated (**Figure 1.4**).

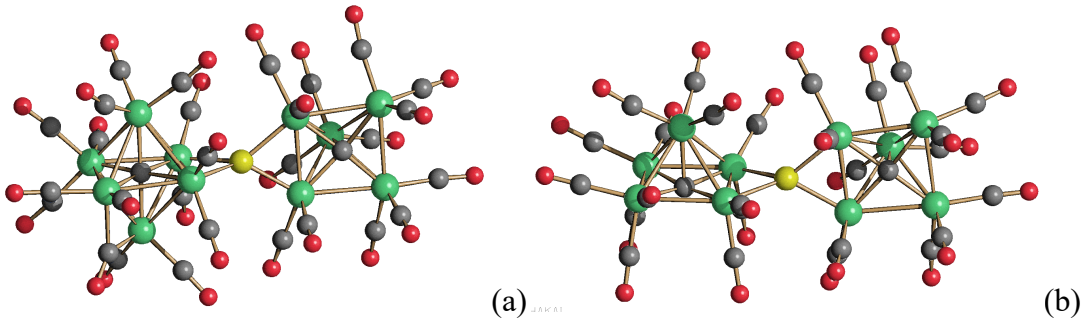

(a) (b)

Figure 1.4 - Molecular structures of (a) $[\{Fe_5(\mu_5\text{-}C)(CO)_{13}\}\{Fe_6(\mu_6\text{-}C)(CO)_{15}\}(\mu_4\text{-}S)]^{2-}$ and (b) $[\{Fe_5(\mu_5\text{-}C)(CO)_{13}\}_2(\mu_4\text{-}S)]^{2-}$ (green, Fe; yellow, S; red, O; grey, C).

1.4 Aim of the Thesis

The aim of this Thesis was to study in detail the oxidation of $[Fe_6C(CO)_{15}]^{4-}$. Indeed, this highly reduced Fe carbide carbonyl cluster is highly reactive and, thus, by carefully controlling the oxidation conditions it could be an interesting starting material for the preparation of new carbide clusters.

Different types of oxidant reagents have been taken into consideration along this work, showing different properties:

- Innocent oxidants, such as $[Cp_2Fe][PF_6]$, which result in the removal of electrons without other complications;
- Strong acids such as $HBF_4{\cdot}Et_2O$, which can act as oxidants through the H^+/H_2 couple as well as being involved in acid-base reactions;
- Alkylating reagents such as the MeI and EtI. These can act as oxidants (see **Paragraph 2.2**), even if more often they are used in order to add a methyl or ethyl group to a substrate;
- S-based reagents including both inorganic reagents such S_8 and S_2Cl_2, and organic reagents such as PhSH. These S-based reagents were mainly employed in the attempt to introduce S-atoms in Fe carbide carbonyl clusters.

All the compounds studied in this Thesis were characterized by IR spectroscopy and, when single crystals were obtained, their structures were determined by single crystal X-ray diffraction (SC-XRD).

2. Results and Discussions

2.1 Synthesis of $[Fe_6C(CO)_{15}]^{4-}$

The compound $[Fe_6C(CO)_{15}]^{4-}$, which is the study object of my thesis, is obtained through a two-step synthesis (**Scheme 2.1**).

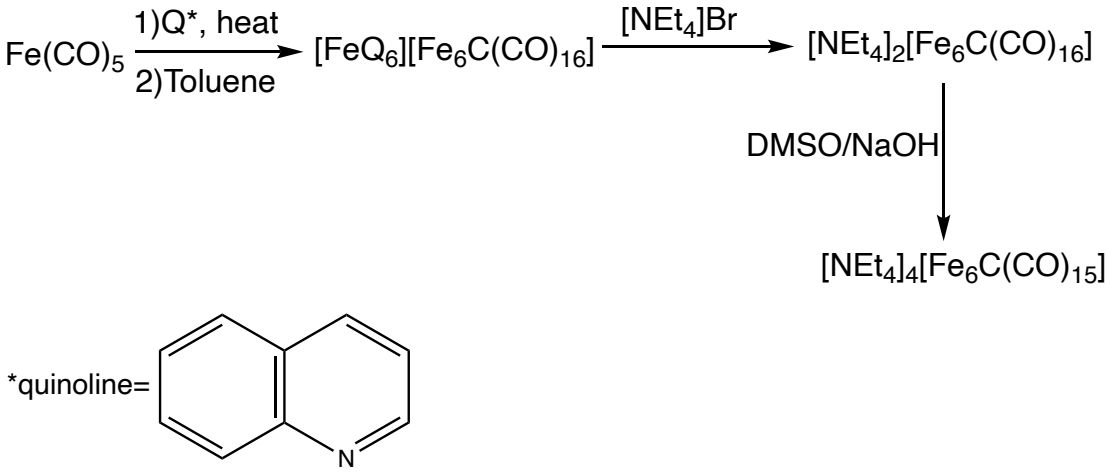

Scheme 2.1 – Two step-synthesis of $[Fe_6C(CO)_{15}]^{4-}$.

The first step of the synthesis consists in the thermal transformation of $Fe(CO)_5$ into $[Fe_6C(CO)_{16}]^{2-}$ upon heating in quinoline (Q) up to 180°C. The second step is the reduction of $[Fe_6C(CO)_{16}]^{2-}$ to $[Fe_6C(CO)_{15}]^{4-}$ with NaOH in DMSO.

Going deeper in the analysis of these two synthetic steps, $Fe(CO)_5$ is heated in quinoline, as mentioned above, and this aromatic heterocyclic compound is characterized by two fundamental properties: it is a high boiling liquid and it is a base.

$Fe(CO)_5$ has an oxidation state number that is equal to zero, and through thermal treatment in the presence of a base such as quinoline, it disproportionates resulting in Fe^{2+} under the form of $[FeQ_6]^{2+}$, and $Fe^{-1/3}$ under the form of $[Fe_6C(CO)_{16}]^{2-}$. Thus, the final product of the reaction is the salt $[FeQ_6][Fe_6C(CO)_{16}]$, which precipitates out of the reaction mixture (**Scheme 2.1**). Thus, one role of quinoline is to coordinate Fe^{2+} favoring the formation of the final product.

Moreover, another point that needs to be outlined in this process is that by using temperatures greater than 160°C, in addition to the disproportionation of the Fe^0, also the disproportionation of the CO to C and CO_2 is obtained (**equation 2.1**).

$$2CO \longrightarrow C + CO_2 \qquad (2.1)$$

The overall reaction is summarized in **equation 2.2**:

$$7\ Fe(CO)_5 + 6\ Q \longrightarrow [FeQ_6]^{2+} + [Fe_6C(CO)_{16}]^{2-} + 18CO + CO_2 \qquad (2.2)$$

Following the experimental procedure, when the reaction stops to produce yellow vapors of $Fe(CO)_5$, it is cooled down to room temperature. Then, toluene is added in order to complete the precipitation of $[FeQ_6][Fe_6C(CO)_{16}]$. After that, the compound of interest is further washed with toluene in order to remove neutral Fe carbonyls present in the reaction mixture. The solid is, then, recovered upon filtration and dried under vacuum.

Extraction with MeOH is performed to have a good separation between the cluster $[Fe_6C(CO)_{16}]^{2-}$ and the abundant metallic Fe that has formed. The main reason whereby this latter is formed concerns the fact that by heating at high T, part of the cluster decomposes giving metallic Fe.

The $[Fe_6C(CO)_{16}]^{2-}$ cluster is precipitated from the MeOH solution as $[NEt_4]^+$ salt through the addition of an aqueous solution of $[NEt_4]Br$ and then the cluster is recovered upon filtration. Different washings with H_2O were done in order to remove all the traces of inorganic salts in order to obtain the pure $[NEt_4]_2[Fe_6C(CO)_{16}]$ salt.

After having analyzed the first stage of the synthesis, the second one is characterized by the reduction reaction of the monocarbide dianion $[Fe_6C(CO)_{16}]^{2-}$ with NaOH in DMSO.

This reaction is well known in organometallic chemistry, and proceeds through a nucleophilic attack of OH^-, given by NaOH, to one coordinated CO ligand forming the intermediate $[Fe_6C(CO)_{15}(COOH)]^{3-}$ in which a carboxylate group is present (**equation 2.3**). The reaction must be carried out in DMSO, because in this polar aprotic solvent the nucleophilic character of NaOH is enhanced.

$$[Fe_6C(CO)_{16}]^{2-} + OH^- \longrightarrow [Fe_6C(CO)_{15}(COOH)]^{3-} \qquad (2.3)$$

The $[Fe_6C(CO)_{15}(COOH)]^{3-}$ intermediate can undergo two different reaction paths, that eventually lead to the same final product (**Figure 2.1)**:

1) It can lose CO_2 with formation of the hydride cluster $[HFe_6C(CO)_{15}]^{3-}$. In turn, this can further react with one OH^- anion, with the consequent removal of a H_2O molecule, and formation of the monocarbide tetraanion $[Fe_6C(CO)_{15}]^{4-}$.
2) Alternatively, the opposite path can be considered. First, $[Fe_6C(CO)_{15}(COOH)]^{3-}$ reacts with OH^- resulting in the elimination of water and formation of $[Fe_6C(CO)_{15}(COO)]^{4-}$. The latter, can lose CO_2 leading to the formation of $[Fe_6C(CO)_{15}]^{4-}$.

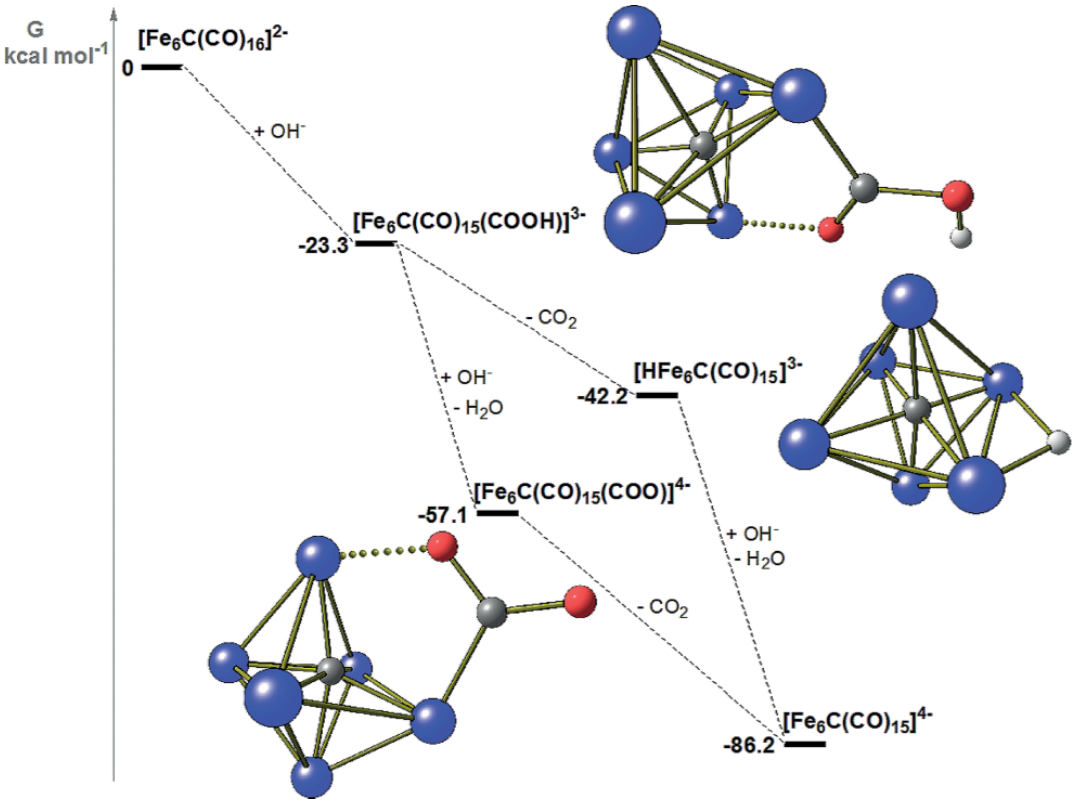

Figure 2.1 – Steps regarding the two pathways that lead to the formation of $[Fe_6C(CO)_{15}]^{4-}$ with the correspondent Relative Gibbs energy values [kcal mol^{-1}] calculated by DFT methods. Color legend: blue Fe, grey C, red O, white H.

The overall reaction leading to the reduction of $[Fe_6C(CO)_{16}]^{2-}$ to $[Fe_6C(CO)_{15}]^{4-}$ is summarized in **equation 2.4**:

$$[Fe_6C(CO)_{16}]^{2-} + 2OH^- \longrightarrow [Fe_6C(CO)_{15}]^{4-} + CO_2 + H_2O \qquad (2.4)$$

The $[Fe_6C(CO)_{15}]^{4-}$ cluster has been characterized through the usage of IR spectroscopy and X-ray diffraction.

The IR spectrum of $[Fe_6C(CO)_{15}]^{4-}$ recorded in MeCN displays two main ν_{CO} bands at 1875(vs) and 1732(m) cm^{-1}, due to terminal and bridging CO ligands, respectively.

While considering the analysis carried out with X-ray diffraction, the molecular structure of this cluster consists of a distorted Fe_6C octahedral cage with 15 CO ligands: one edge bridging, four semi-bridging and ten terminal carbonyls as shown in **Figure 2.2**.

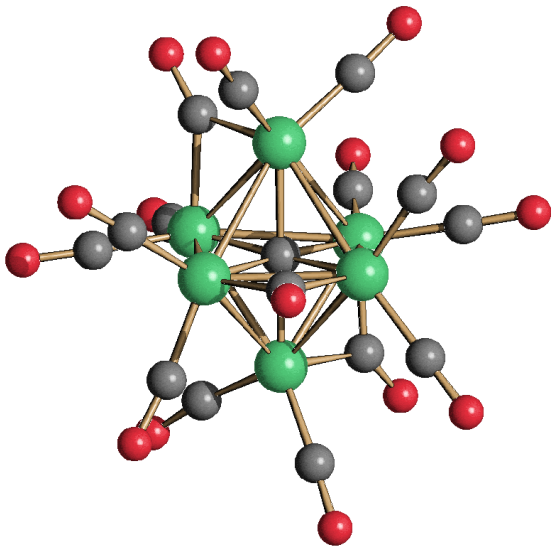

Figure 2.2 – Molecular structure of $[Fe_6C(CO)_{15}]^{4-}$ (green Fe, red O, grey C).

2.2 Oxidation of $[Fe_6C(CO)_{15}]^{4-}$: General features

The oxidation of the highly reduced species $[Fe_6C(CO)_{15}]^{4-}$ was studied in details using different oxidants ($[Cp_2Fe][PF_6]$, $HBF_4{\cdot}Et_2O$, MeI and EtI), different stoichiometries and experimental conditions. It must be remarked that the formal oxidation number of Fe in $[Fe_6C(CO)_{15}]^{4-}$ is -0.67.

$[Cp_2Fe][PF_6]$ is an innocent one-electron oxidant, in accord to **equation 2.5**. Indeed, $[Cp_2Fe]^+$ is a 17-electron species that is transformed into the 18-electron Cp_2Fe upon acquisition of one electron. The use of $[PF_6]^-$ as counter-ion increases the solubility in organic solvents. Moreover, this is a stable and poorly coordinating anion and, therefore, it is very unlikely its involvement in side-reactions.

$$[Cp_2Fe]^+ + e^- \rightleftharpoons [Cp_2Fe] \quad (2.5)$$

Another type of oxidant used during this screening was $HBF_4 \cdot Et_2O$. This is a strong acid, soluble in organic solvents and containing the weakly coordinating anion $[BF_4]^-$. Moreover, this is commercially available as Et_2O solution, thus, avoiding the presence of water. Dissociation of $HBF_4 \cdot Et_2O$ results in H^+ cations and $[BF_4]^-$ anions in accordance to **equation 2.6.**

$$HBF_4 \longrightarrow H^+ + BF_4^- \quad (2.6)$$

The oxidation capacity of $HBF_4 \cdot Et_2O$ is due to the H^+/H_2 couple as depicted in the semi-reaction reported as **equation 2.7.**

$HBF_4 \cdot Et_2O$ as an oxidant:

$$H^+ + e^- \rightleftharpoons 1/2\ H_2 \quad (2.7)$$

In addition, $HBF_4 \cdot Et_2O$ may behave as an acid toward the cluster, which may accept a H^+ ion, in accord to **equation 2.8**. Protonation of an anionic metal carbonyl cluster may occur at the O-atom of a CO ligand or at the metal cage. The latter reaction is the one more often observed, which leads to the formation of metal hydride carbonyl clusters.

$HBF_4 \cdot Et_2O$ as an acid toward the cluster:

$$H^+ + B \rightleftharpoons BH^+ \qquad B = [Fe_6C(CO)_{15}]^{4-} \quad (2.8)$$

The last two oxidants used during this screening were MeI and EtI, which have similar properties and may be viewed as RI alkylating agents. Indeed, these are often used in order to donate a R^+ cation to a nucleophile in accordance to **equation 2.9**. In the case of an anionic metal carbonyl cluster, the nucleophilic site is usually represented by the oxygen of a CO ligand resulting in an alkoxy-carbyne $[C\text{-}O\text{-}R]^+$ group.

MeI as an alkylating agent:

$$MeI + Nu \longrightarrow MeNu^{+} + I^{-} \qquad (2.9)$$

Even if it is rarer, RI species such as MeI may also operate as oxidants. This formally involves the one-electron reduction of the Me^{+} cation that results in a methyl radical as depicted in **equation 2.10** . The fate of this radical depends, then, on the experimental conditions. It may, for instance, react with the substrate or the solvent, or alternatively dimerize to give ethane.

MeI as an oxidant:

$$MeI + e^{-} \longrightarrow Me^{\bullet} + I^{-} \qquad (2.10)$$

As a general procedure, a solution of the oxidant ($[Cp_2Fe][PF_6]$, $HBF_4 \cdot Et_2O$, MeI or EtI) in MeCN was added dropwise to a solution of $[Fe_6C(CO)_{15}]^{4-}$ in MeCN and the reactions monitored by IR spectroscopy. At the end of the reaction, the solvent was removed under vacuum and the residue washed with H_2O in order to remove inorganic salts. The different products were separated by extraction with organic solvents of increasing polarity (toluene, THF, acetone, MeCN) and analyzed by IR spectroscopy. When new products were isolated, their crystallization was attempted by slow diffusion of a non-solvent into their solutions.

After screening different experimental conditions, it is possible to outline a general scheme for the oxidation of $[Fe_6C(CO)_{15}]^{4-}$ (**Scheme 2.2**)

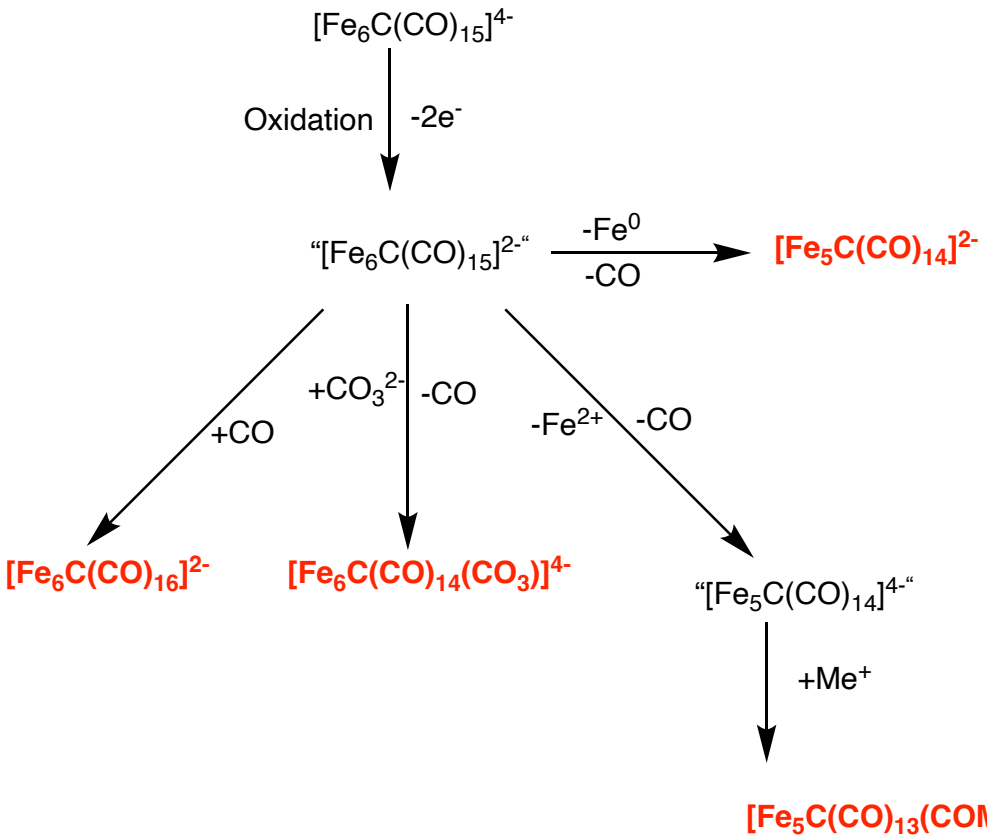

Scheme 2.2 - General view of the oxidation of $[Fe_6C(CO)_{15}]^{4-}$. Species reported in red have been isolated and structurally characterized.

It must be remarked that often the oxidation of $[Fe_6C(CO)_{15}]^{4-}$ leads to a mixture of products. By carefully controlling the experimental conditions, a slightly higher selectivity may be obtained but, in all cases, some separation procedures (see above) may be adopted in order to isolate pure products. This behavior may be explained assuming that the first step of the oxidation of $[Fe_6C(CO)_{15}]^{4-}$ is the formation of a purported "$[Fe_6C(CO)_{15}]^{2-}$" unsaturated species by removal of two electrons from the former. Herein, "saturated" and "unsaturated" refer to the fact that, based on the Wade-Mingos rules, an octahedral cluster should possess 86 cluster valence electrons (CVE). Thus, $[Fe_6C(CO)_{15}]^{4-}$ is a saturated cluster possessing 86 CVE [8×6 (6 Fe) + 4×1 (C) + 2×15 (15 CO) + 4 (anionic charge)], whereas the purported "$[Fe_6C(CO)_{15}]^{2-}$" is unsaturated possessing 84 CVE [8×6 (6 Fe) + 4×1 (C) + 2×15 (15 CO) + 2 (anionic charge)].

It must be remarked that there is no experimental evidence for the formation of "$[Fe_6C(CO)_{15}]^{2-}$". Nonetheless, its formation as an intermediate explains very well all the other products experimentally observed and isolated. Moreover, similar studies on analogous ruthenium clusters, carried out by the research group where I did my Thesis, have clearly shown

that the oxidation of $[Ru_6C(CO)_{15}]^{4-}$ results firstly on $[Ru_6C(CO)_{15}]^{2-}$, which has been spectroscopically observed. Moreover, also spectroelectrochemical studies have given support to the formation of the unsaturated cluster $[Ru_6C(CO)_{15}]^{2-}$ upon electrochemical oxidation of $[Ru_6C(CO)_{15}]^{4-}$. Finally, the related unsaturated hydride $[HRu_6C(CO)_{15}]^{-}$ has been structurally characterized by single-crystal X-ray diffraction.

Due to its high instability, the purported "$[Fe_6C(CO)_{15}]^{2-}$" species rapidly decomposes, mainly leading to iron metal and free CO gas. The latter gas may react with further "$[Fe_6C(CO)_{15}]^{2-}$" leading to the saturated species $[Fe_6C(CO)_{16}]^{2-}$, that is often observed as main product or side product of the oxidation process. This compound has been identified by IR spectroscopy and X-ray crystallography. In general, $[Fe_6C(CO)_{16}]^{2-}$ represents the major product of the reaction when an innocent oxidant such as $[Cp_2Fe][PF_6]$ is employed. Formation of $[Fe_6C(CO)_{16}]^{2-}$ may be taken as an indirect proof of the formation of "$[Fe_6C(CO)_{15}]^{2-}$" as an intermediate of the reaction.

Looking at the IR spectra of the latter species, it is characterized by the following ν_{CO} bands: 2028(w), 2002 (w), 1963(vs), 1766(w) cm^{-1}.

This hypothesis is further supported by the fact that performing the oxidation of $[Fe_6C(CO)_{15}]^{4-}$ in the presence of a trapping agent such as Na_2CO_3, the species $[Fe_6C(CO)_{14}(CO_3)]^{4-}$ is formed (see **Paragraph 2.3** for further details). This may be viewed as the product of the addition of a carbonate ion to the purported "$[Fe_6C(CO)_{15}]^{2-}$" species with concomitant loss of one CO ligand.

When $HBF_4{\cdot}Et_2O$ is used to oxidize $[Fe_6C(CO)_{15}]^{4-}$, beside $[Fe_6C(CO)_{16}]^{2-}$, often the penta-nuclear species $[Fe_5C(CO)_{14}]^{2-}$ is obtained. This represents the major product of the oxidation when the acid is employed. Formation of $[Fe_5C(CO)_{14}]^{2-}$ formally arises from loss of one Fe(0) atom and one CO ligand from the "$[Fe_6C(CO)_{15}]^{2-}$" intermediate. It is likely that H^+ ions further oxidize Fe(0) to Fe(II) favoring the formation of $[Fe_5C(CO)_{14}]^{2-}$. This penta-nuclear cluster has been identified by IR spectroscopy (**Figure 2.3**) by comparison to literature data. Moreover, its molecular structure has been ascertained by X-ray crystallography as $[NEt_4]_2[Fe_5C(CO)_{14}]$ salt (**Figure 2.4**). The cluster is composed of a square-pyramidal Fe_5C core, with the unique carbide atom in a semi-exposed position at the center of the square base of the metal cage. It contains 13 terminal CO ligands and one edge bridging μ-CO ligand on one of the edges of the base of the pyramid.

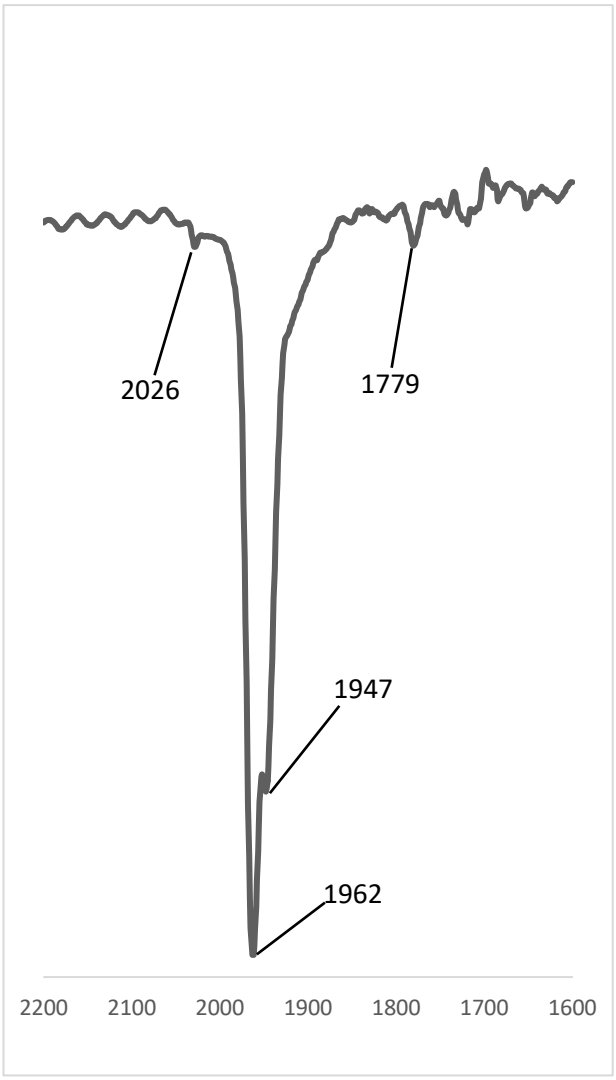

Figure 2.3 - IR spectrum in the ν_{CO} region of $[Fe_5C(CO)_{14}]^{2-}$ recorded in THF. All the reported values are in cm^{-1}.

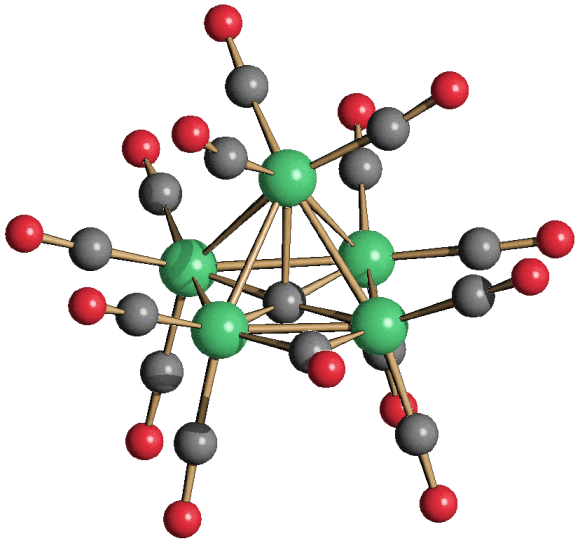

Figure 2.4 - Molecular structure of $[Fe_5C(CO)_{14}]^{2-}$ (green, Fe; red, O; grey, C).

When MeI is employed for the oxidation of $[Fe_6C(CO)_{15}]^{4-}$, beside $[Fe_6C(CO)_{16}]^{2-}$ also the new cluster $[Fe_5C(CO)_{13}(COMe)]^{3-}$ is obtained. Moreover, in the presence of Na_2CO_3, also some $[Fe_6C(CO)_{14}(CO_3)]^{4-}$ may be formed. Formation of $[Fe_5C(CO)_{13}(COMe)]^{3-}$ may be formally accounted for assuming that the "$[Fe_6C(CO)_{15}]^{2-}$" intermediate eliminated one Fe(II) ion and one CO ligands affording a purported "$[Fe_5C(CO)_{14}]^{4-}$" species, which is then methylated to give $[Fe_5C(CO)_{13}(COMe)]^{3-}$. Details on the formation and characterization of this new product will be reported in the next Section.

2.3 Reactions of $[Fe_6C(CO)_{15}]^{4-}$ with MeI

As outlined in the **Paragraph 2.2**, the reaction of $[Fe_6C(CO)_{15}]^{4-}$ with MeI results in a mixture of $[Fe_6C(CO)_{16}]^{2-}$ and $[Fe_5C(CO)_{13}(COMe)]^{3-}$ (**Scheme 2.3**). The two compounds can be separated owing their different solubility in organic solvents. Thus, $[Fe_6C(CO)_{16}]^{2-}$ can be extracted in THF, whereas $[Fe_5C(CO)_{13}(COMe)]^{3-}$ is soluble in MeCN.

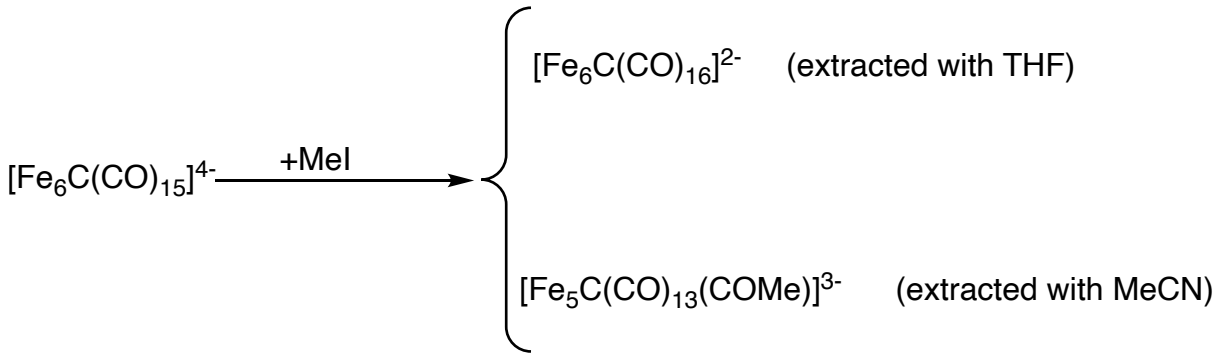

Scheme 2.3 - Reaction of $[Fe_6C(CO)_{15}]^{4-}$ with MeI.

Interestingly, performing the reaction between $[Fe_6C(CO)_{15}]^{4-}$ and MeI in the presence of Na_2CO_3, a third compound besides $[Fe_6C(CO)_{16}]^{2-}$ and $[Fe_5C(CO)_{13}(COMe)]^{3-}$ is obtained, that is, $[Fe_6C(CO)_{14}(CO_3)]^{4-}$ (**Scheme 2.4**). Also in this case, the different products can be separated by extraction with organic solvents of increasing polarity, that is, $[Fe_6C(CO)_{16}]^{2-}$ with THF, $[Fe_6C(CO)_{14}(CO_3)]^{4-}$ with acetone, and $[Fe_5C(CO)_{13}(COMe)]^{3-}$ with MeCN. The proposed mechanism for the formation of the different products is reported in **Paragraph 2.2**. All the clusters have been characterized by IR spectroscopy and their structures determined by single crystal X-ray diffraction (SC-XRD).

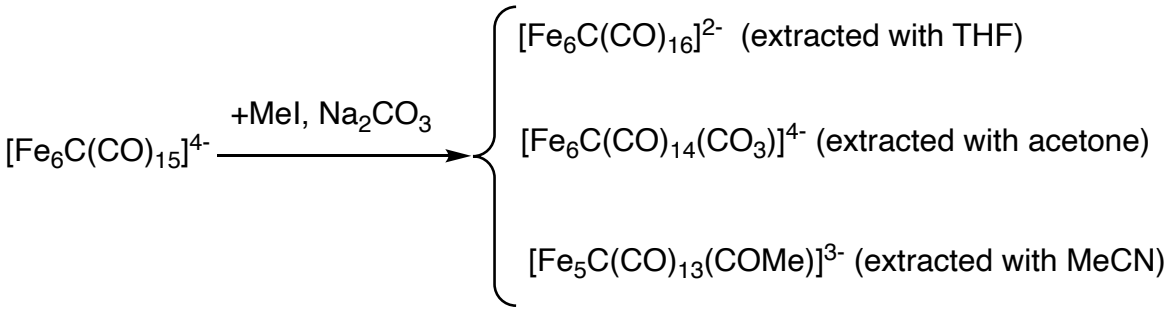

Scheme 2.4 - Reaction of $[Fe_6C(CO)_{15}]^{4-}$ with MeI in the presence of Na_2CO_3.

The compound $[Fe_6C(CO)_{16}]^{2-}$ is already known in the literature and, indeed, it is the starting product for the synthesis of $[Fe_6C(CO)_{15}]^{4-}$ as described in **Paragraph 2.1**. It shows typical ν_{CO} bands at 1966(s) and 1776(w) cm^{-1} for the terminal and edge bridging carbonyls, respectively. These are moved at higher wavenumbers compared to $[Fe_6C(CO)_{15}]^{4-}$ (1875(vs), 1732(m) cm^{-1}) due to the reduced negative charge. The molecular structure of $[Fe_6C(CO)_{16}]^{2-}$ is based on an octahedral Fe_6C cage centered by the unique carbide atom (**Figure 2.5**). It contains 13 terminal and 3 edge bridging CO ligands.

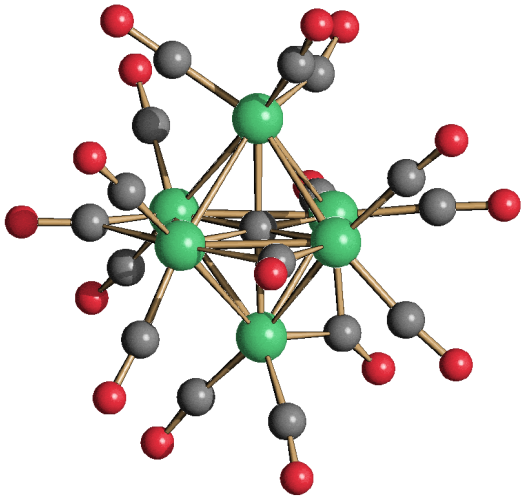

Figure 2.5 - Molecular structure of $[Fe_6C(CO)_{16}]^{2-}$ (green Fe, red O, grey C)

The new cluster $[Fe_5C(CO)_{13}(COMe)]^{3-}$ displays ν_{CO} bands at 1921(vs) and 1793(w) cm^{-1} for terminal and bridging carbonyls, respectively (**Figure 2.6**). The ν_{CO} bands of $[Fe_5C(CO)_{13}(COMe)]^{3-}$ appear at intermediate wavenumbers between those of $[Fe_6C(CO)_{16}]^{2-}$ and $[Fe_6C(CO)_{15}]^{4-}$, because of the intermediate anionic charge.

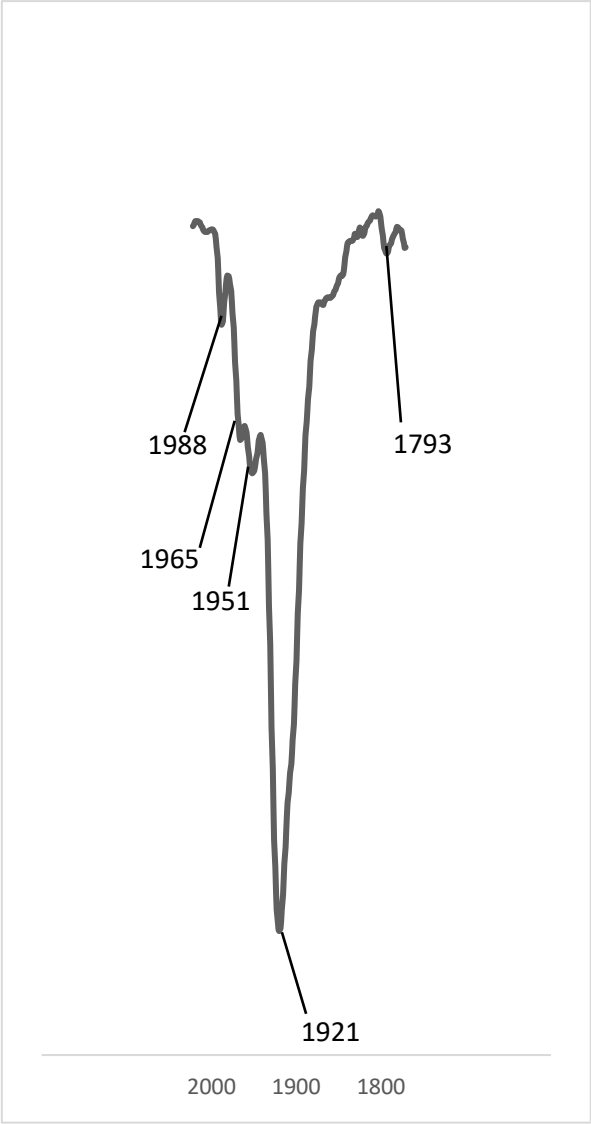

Figure 2.6 - IR spectrum in the ν_{CO} region of $[Fe_5C(CO)_{13}(COMe)]^{3-}$ recorded in MeCN.

The molecular structure of $[Fe_5C(CO)_{13}(COMe)]^{3-}$ is closely related to that of $[Fe_5C(CO)_{14}]^{2-}$ described in the previous Paragraph, being based on the same square-pyramidal Fe_5C core. The carbide atom is in a semi-exposed position, whereas the unique acetyl –COMe group is terminally bonded to one Fe atom of the square base of the cluster. The two edges of the square base adjacent to the Fe-COMe group are bridged by two μ-CO ligands, whereas the remaining 11 carbonyls are in terminal positions (**Figure 2.7**).

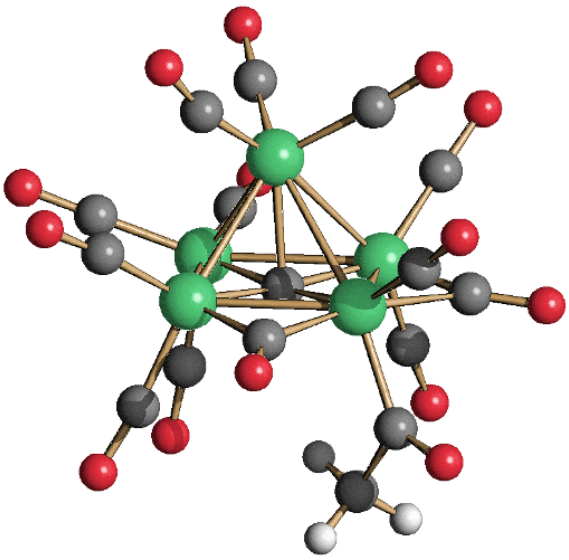

Figure 2.7 - Molecular structure of the anion $[Fe_5C(CO)_{13}(COMe)]^{3-}$ (green Fe, red O, grey C, white H).

The new compound $[Fe_6C(CO_{14})(CO_3)]^{4-}$ is often obtained as side product when the oxidation of $[Fe_6C(CO)_{15}]^{4-}$ is carried out in the presence of Na_2CO_3. It is partially separated by the other products by extraction with acetone. Crystals suitable for SC-XRD analyses of $[NEt_4]_3[H_3O][Fe_6C(CO_{14})(CO_3)]$ have been obtained by slow diffusion on n-hexane into the acetone solution of $[Fe_6C(CO_{14})(CO_3)]^{4-}$, allowing its full structural characterization (**Figure 2.8**). The structure of the cluster is characterized by an octahedral geometry, composed of a metallic core in which are present 6 Fe atoms with a carbide located in the center. There are 12 terminal and two edge bridging CO ligands. Moreover, there is a CO_3^{2-} anion bonded through two O-atoms to a single Fe atom. In the solid state, there is an hydrogen bond between the third oxygen of the carbonate group and the $[H_3O]^+$ cation present in the unit cell.

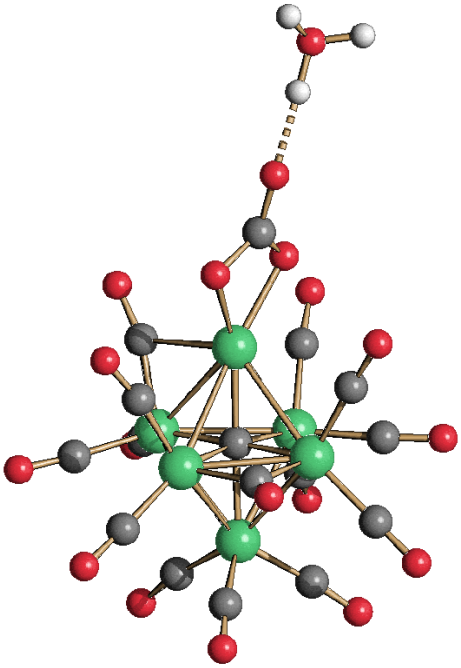

Figure 2.8 - Molecular structure of $[Fe_6C(CO)_{14}(CO_3)]^{4-}$ showing the H-bond with the $[H_3O]^+$ cation as a fragmented line (green, Fe; red, O; grey, C; white H).

The IR spectrum of $[Fe_6C(CO)_{14}(CO_3)]^{4-}$ recorded in an acetone solution displays the main ν_{CO} band at 1947 cm^{-1}. This is an intermediate value between those of $[Fe_6C(CO)_{16}]^{2-}$ (1966 cm^{-1}) and $[Fe_6C(CO)_{15}]^{4-}$ (1875 cm^{-1}), suggesting that the cluster assumes a 3- charge in solution. This could be explained by assuming that protonation of the coordinated carbonate ligand occurs in solution resulting in $[Fe_6C(CO_{14})(HCO_3)]^{3-}$. This would correspond to the transfer of a proton from $[H_3O]^+$ to the cluster.

Looking at the IR spectrum of the latter species, this is characterized by the following ν_{CO} bands: 2015(w), 1947(vs), 1785(w) cm^{-1}.

2.4 Reactions of $[Fe_6C(CO)_{15}]^{4-}$ with S-based reagents

Due to the great interest present in the literature for Fe carbide clusters containing inorganic or organic sulphur as potential models for the nitrogenase cofactor, a preliminary study aimed at introducing S-atoms in $[Fe_6C(CO)_{15}]^{4-}$ was carried out. This study was based on the analysis of the reactivity of $[Fe_6C(CO)_{15}]^{4-}$ in the presence of organic or inorganic molecules containing sulphur, that is, S_8, S_2Cl_2 and PhSH.

Considering the cases of S_8 and S_2Cl_2, oxidation of $[Fe_6C(CO)_{15}]^{4-}$ takes place following a path similar to that observed in **Paragraphs 2.2** and **2.3** with other oxidants. Most of the time, the main product coming from the reactions carried out by using these two S-based oxidants is $[Fe_6C(CO)_{16}]^{2-}$ with evidence of some further by-products different from those seen previously; unfortunately, it has not been possible to isolate and characterize these species.

Conversely, the reactions carried out using PhSH resulted in a mixture of products, as can be seen from **Scheme 2.5**.

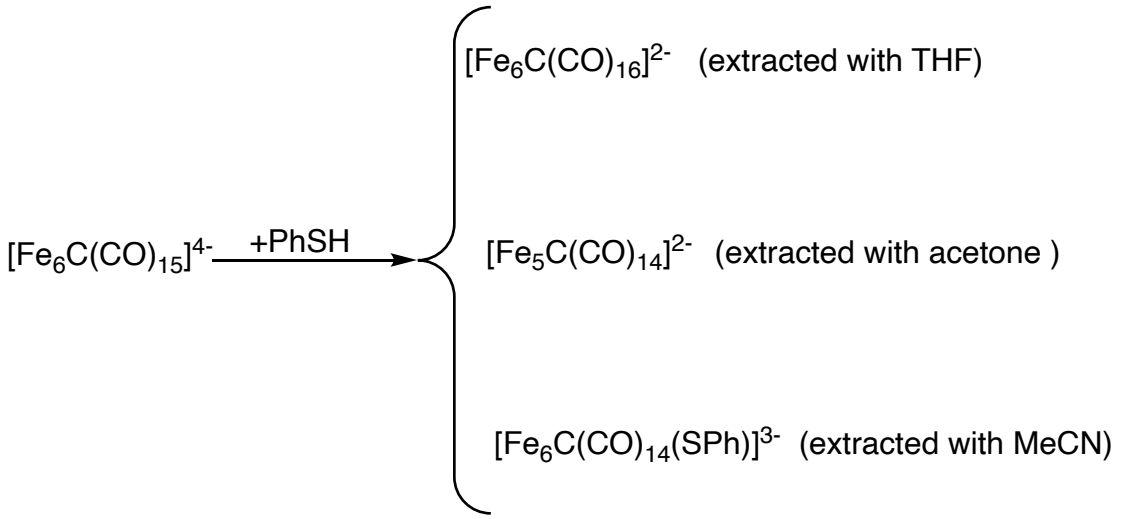

Scheme 2.5 - Reaction of $[Fe_6C(CO)_{15}]^{4-}$ with PhSH.

All these products were partially separated by extraction with organic solvent with increasing polarity. Considering $[Fe_6C(CO)_{16}]^{2-}$ and $[Fe_5C(CO)_{14}]^{2-}$, both these products result from the oxidation of $[Fe_6C(CO)_{15}]^{4-}$ as reported in the previous paragraph (**Paragraph 2.2**), whereas $[Fe_6C(CO)_{14}(SPh)]^{3-}$ is a new compound coming from this synthesis.

The formation of $[Fe_6C(CO)_{14}(SPh)]^{3-}$ can be explained following an oxidative mechanism similar to that reported in **Paragraph 2.2** that involves a purported "$[Fe_6C(CO)_{15}]^{2-}$" intermediate (**Scheme 2.6**).

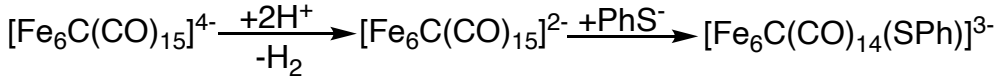

Scheme 2.6 – Formation of $[Fe_6C(CO)_{14}(SPh)]^{3-}$

Indeed, PhSH is a weak acid that in solution partially dissociates to H^+ and PhS^- as depicted in equation (**2.11**).

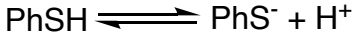

(2.11)

The H^+ ion is able to oxidize $[Fe_6C(CO)_{15}]^{4-}$ reducing itself to H_2, as previously seen in the case of $HBF_4 \cdot Et_2O$ (**Paragraph 2.2**).

The oxidation of the cluster leads to the formation of "$[Fe_6C(CO)_{15}]^{2-}$" which is the unstable and unsaturated species claimed to be involved in all the oxidation processes described in this Thesis. This monocarbide dianionic cluster is able to capture the PhS^- formed from the dissociation of PhSH following equation (**2.11)**, resulting in the observed cluster $[Fe_6C(CO)_{14}(SPh)]^{3-}$.

The mechanism for the formation of $[Fe_6C(CO)_{14}(SPh)]^{3-}$ is quite similar to the one described for $[Fe_6C(CO)_{14}(CO_3)]^{4-}$ (**Paragraph 2.3**), where "$[Fe_6C(CO)_{15}]^{2-}$" reacted with CO_3^{2-} instead of PhS^-.

The new cluster $[Fe_6C(CO)_{14}(SPh)]^{3-}$ was analyzed and characterized through IR spectroscopy and single crystal X-ray diffraction (SC-XRD).

The IR spectrum of $[Fe_6C(CO)_{14}(SPh)]^{3-}$ (**Figure 2.9**) displays a ν_{CO} band (1911 cm^{-1}) at higher wavenumbers compared to $[Fe_6C(CO)_{15}]^{4-}$ (1872 cm^{-1}) in view of its reduced anionic charge. It must be remarked that the IR spectrum reported in **Figure 2.9** is actually a mixture of $[Fe_6C(CO)_{14}(SPh)]^{3-}$ (ν_{CO} 1911 cm^{-1}) and $[Fe_6C(CO)_{15}]^{4-}$ (ν_{CO} 1872 cm^{-1}).

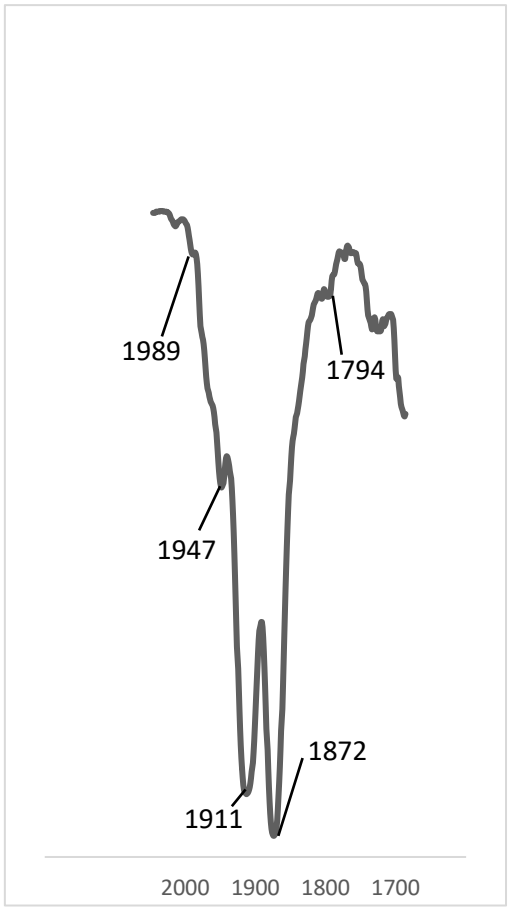

Figure 2.9 - IR spectrum in the ν_{CO} region of $[Fe_6C(CO)_{14}(SPh)]^{3-}$ (ν_{CO} 1911 cm^{-1}) recorded in MeCN with the presence of unreacted $[Fe_6C(CO)_{15}]^{4-}$ (ν_{CO} 1872 cm^{-1}).

The molecular structure of $[Fe_6C(CO)_{14}(SPh)]^{3-}$ (**Figure 2.10**) is based on an octahedral Fe_6C core as the parent $[Fe_6C(CO)_{15}]^{4-}$. The PhS^- anion bridges one Fe-Fe edge of the octahedron. There are 10 terminal, 2 edge bridging and 2 semi-bridging CO ligands. The μ-SPh ligand formally donates 3 electrons and, thus, it replaces one CO and one negative charge compared the parent $[Fe_6C(CO)_{15}]^{4-}$, resulting in the final formula $[Fe_6C(CO)_{14}(SPh)]^{3-}$.

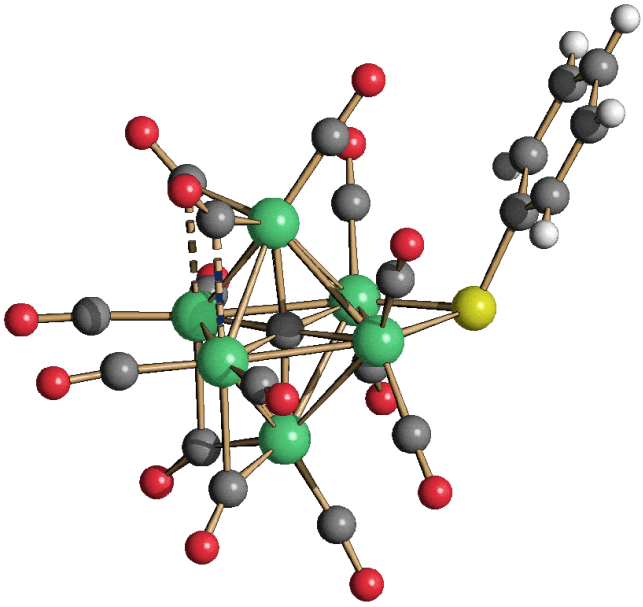

Figure 2.10 - Molecular structure of $[Fe_6C(CO)_{14}(SPh)]^{3-}$ (green, Fe; yellow, S; red, O; grey, C; white, H).

3. Conclusions

The first target of my Internship concerned the detailed investigation of the oxidation of the highly reduced carbide carbonyl cluster $[Fe_6C(CO)_{15}]^{4-}$. By employing different oxidants ($[Cp_2Fe][PF_6]$, $HBF_4{\cdot}Et_2O$, MeI and EtI) and carefully controlling the experimental conditions, it was possible to depict a general mechanism for this process. Thus, $[Fe_6C(CO)_{15}]^{4-}$ is at first oxidized to give a purported highly unstable species formulated as "$[Fe_6C(CO)_{15}]^{2-}$", based on analogous studies on related ruthenium clusters. This "$[Fe_6C(CO)_{15}]^{2-}$" intermediate species rapidly evolves to give different products, among which the previously reported $[Fe_6C(CO)_{16}]^{2-}$ and $[Fe_5C(CO)_{12}]^{2-}$ have been often observed. These are the main products obtained by using $[Cp_2Fe][PF_6]$ and $HBF_4{\cdot}Et_2O$ as oxidants. Conversely, by using MeI, the formation of $[Fe_6C(CO)_{16}]^{2-}$ is accompanied by the new clusters $[Fe_5C(CO)_{13}(COMe)]^{3-}$.

Moreover, in the presence of a trapping agent such as Na_2CO_3, also formation of $[Fe_6C(CO)_{14}(CO_3)]^{4-}$ was observed as an additional product.

The second target of my work concerned the insertion of S-atoms within Fe carbide carbonyl clusters. Using inorganic S-sources such as S_8 and S_2Cl_2, the target was not achieved, since only oxidation of $[Fe_6C(CO)_{15}]^{4-}$ was observed. Conversely, using the organic compound PhSH, incorporation of sulphur within the cluster $[Fe_6C(CO)_{14}(SPh)]^{3-}$ was successfully obtained. This species was obtained in mixture with previously reported $[Fe_6C(CO)_{16}]^{2-}$ and $[Fe_5C(CO)_{12}]^{2-}$.

All the species were characterized by IR spectroscopy. Moreover, the molecular structures of the new clusters $[Fe_5C(CO)_{13}(COMe)]^{3-}$, $[Fe_6C(CO)_{14}(CO_3)]^{4-}$ and $[Fe_6C(CO)_{14}(SPh)]^{3-}$, as well as confirmation of the structures of the previously reported $[Fe_5C(CO)_{14}]^{2-}$ and $[Fe_6C(CO)_{16}]^{2-}$, were performed by SC-XRD.

Further studies will be devoted to the use of different organic molecules as sulphur sources in order to widen the scope of this work, including different thiols (RSH) and di-sulfides (RSSR).

4. Experimental part

4.1 General Procedures

All reactions and sample manipulations were carried out using standard Schlenk techniques under nitrogen and in dried solvents.

The solvents used (CH_2Cl_2, MeCN, acetone, DMF, DMSO, MeOH, EtOH, toluene, n-hexane, H_2O, diisopropyl ether) were degassed and stored under nitrogen atmosphere. The solvent THF was distillated on Na/Benzophenone and stored under nitrogen.

The following reagents were used as received without any further purifications: MeI, EtI, $HBF_4 \cdot Et_2O$, Na_2CO_3, S_8, S_2Cl_2, PhSH

IR spectra were recordedon a Perkin Elmer Spectrum One interferometer in CaF_2 cells.

The molecular structure were determined by single crystal X-ray diffraction. The diffraction experiments were carried out on a Bruker APEX II diffractometer equipped with a PHOTON2 detector using Mo–Kα radiation.

4.2 Synthesis of $[NEt_4]_4[Fe_6C(CO)_{15}]$

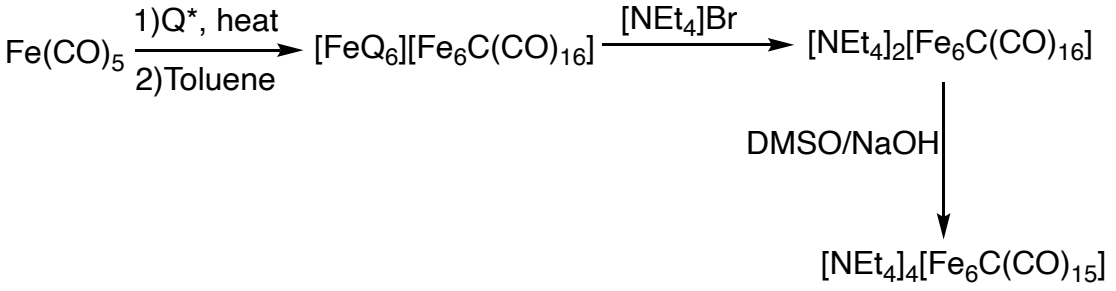

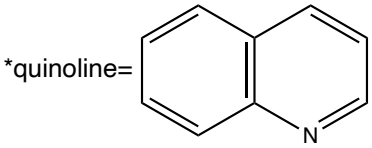

$Fe(CO)_5$ (15 mL, 111 mmol) and quinoline (15 mL, 127 mmol) were introduced in a 100 mL two-necked round-bottom flask under nitrogen. The reaction mixture was gradually heated up to 180 °C in 2 h and, then, maintained at 180 °C for 4 h. When the yellow vapors of $Fe(CO)_5$

stopped to form, the reaction was stopped and cooled down to room temperature. Toluene (50 mL) was added to the reaction mixture in order to precipitate $[FeQ_6][Fe_6C(CO)_{16}]$, which was recovered upon filtration and washed with toluene (3 × 50 mL). The solid was dried under reduced pressure and $[FeQ_6][Fe_6C(CO)_{16}]$ extracted in MeOH (4 × 50 mL) in order to separate it from metallic Fe. After filtration, the volume of the solution was reduced from 200 to 50 mL under vacuum. Metathesis of the cation was obtained by adding a saturated solution of $[NEt_4]Br$ in H_2O (100 mL) to the MeOH solution. Precipitation of $[NEt_4]_2[Fe_6C(CO)_{16}]$ was completed by addition of H_2O (100 mL). The solid was recovered upon filtration, washed with H_2O (3 × 50 mL) and dried under vacuum.

The so obtained $[NEt_4]_2[Fe_6C(CO)_{16}]$ was dissolved in DMSO (40 mL) in a Schlenk tube and, then, solid NaOH (1.65 g, 41.2 mmol) was added. The reaction mixture was stirred under nitrogen for 4 days and the progress of the reaction monitored by IR spectroscopy. At the end of the reaction the ν_{CO} bands of the starting $[Fe_6C(CO)_{16}]^{2-}$ (1966 cm^{-1}) disappeared and were replaced by those of $[Fe_6C(CO)_{15}]^{4-}$ (1875 cm^{-1}). NaOH was mechanically removed and $[NEt_4]_4[Fe_6C(CO)_{15}]$ precipitated out of the reaction mixture upon addition of a saturated solution of $[NEt_4]Br$ in H_2O (100 mL) and, then, pure H_2O (100 mL). Solid $[NEt_4]_4[Fe_6C(CO)_{15}]$ was recovered upon filtration and washed with H_2O (2 × 50 mL), toluene (2 × 50 mL), THF (2 × 50 mL), and acetone (2 × 50 mL). The product was dried under vacuum, extracted in MeCN, and used as starting material in all the following reactions.

Characterization of $[NEt_4]_4[Fe_6C(CO)_{15}]$:

IR (MeCN, 293 K) ν_{CO}: 1875(vs), 1732(m) cm^{-1}

4.3 Reaction of $[NEt_4]_4[Fe_6C(CO)_{15}]$ with MeI in the presence of Na_2CO_3: Synthesis of $[NEt_4]_3[Fe_5C(CO)_{13}(COMe)]$

$$[NEt_4]_4[Fe_6C(CO)_{15}] \xrightarrow[MeCN,\ Na_2CO_3]{MeI} [NEt_4]_3[Fe_5C(CO)_{13}(COMe)]$$

$[NEt_4]_4[Fe_6C(CO)_{15}]$ (0.37 g, 0.288 mmol) was solubilized in MeCN (20 mL) and then, Na_2CO_3 (6.08 mg, 0.057 mmol) was added. A solution of MeI (304 μL, 4.90 mmol) in MeCN (5 mL) was prepared, and added to the solution of the cluster in three portions (0.2 mL, 0.2 mL and 0.1

mL). At the end of the reaction, there was IR evidence of the presence in the solution of $[Fe_6C(CO)_{16}]^{2-}$ (ν_{CO} 1966 cm^{-1}) and $[Fe_5C(CO)_{13}(COMe)]^{3-}$ (ν_{CO} 1917 cm^{-1}).
The solvent was evaporated under vacuum and the solid was washed with H_2O (20 mL) and toluene (20 mL).
$[NEt_4]_2[Fe_6C(CO)_{16}]$ was removed from the solid residue with THF (10 mL), whereas the extraction in acetone (10 mL) contained a minor amount of $[NEt_4]_2[Fe_6C(CO)_{16}]$ together with a major product showing ν_{CO} at 1917 cm^{-1} which was attributable to a purported species $[NEt_4]_4[Fe_6C(CO)_{14}(CO_3)]$. The residue was, then, extracted with MeCN (10 mL) and the resulting solution showed a ν_{CO} at 1920 cm^{-1} which was attributable to a purported species $[NEt_4]_3[Fe_5C(CO)_{13}(COMe)]$.

Characterization of $[NEt_4]_4[Fe_6C(CO)_{14}(CO_3)]$:
IR (acetone,298K) ν_{CO}: 2015 (w), 1947 (vs), 1785 (w) cm^{-1}

Characterization of $[NEt_4]_3[Fe_5C(CO)_{13}(COMe)]$:
IR (MeCN, 298K) ν_{CO}: 1988(w),1920(s), 1793(w) cm^{-1}

4.4 Reaction of $[NEt_4]_4[Fe_6C(CO)_{15}]$ with MeI: Synthesis of $[NEt_4]_3[Fe_5C(CO)_{13}(COMe)]$

$$[NEt_4]_4[Fe_6C(CO)_{15}] \xrightarrow[MeCN]{MeI} [NEt_4]_3[Fe_5C(CO)_{13}(COMe)]$$

$[NEt_4]_4[Fe_6C(CO)_{15}]$ (0.35 g, 0.272 mmol) was solubilized in MeCN (25 mL). A solution of MeI (304 μL, 4.90 mmol) in MeCN (5 mL) was prepared, and only 0.5 mL of the total 5 mL were added to the cluster solution.
At the end of the reaction, there was IR evidence of the presence in the solution of $[NEt_4]_2[Fe_6C(CO)_{16}]$ (ν_{CO} 1965 cm^{-1}) and $[NEt_4]_3[Fe_5C(CO)_{13}(COMe)]$ (ν_{CO} 1916 cm^{-1}).
The solvent was evaporated under vacuum and the solid was washed with H_2O (20 mL) and toluene (20 mL).
$[NEt_4]_2[Fe_6C(CO)_{16}]$ was removed from the solid residue with THF (20 mL), whereas the extraction in acetone (10 mL) contained a minor amount of $[Fe_5C(CO)_{14}]^{2-}$ showing ν_{CO} bands at 1963 and 1947 cm^{-1} together with the presence of a product showing ν_{CO} at 1920 cm^{-1} which was attributable to a purported species $[NEt_4]_3[Fe_5C(CO)_{13}(COMe)]$.

The residue was, then, extracted with MeCN (10 mL) and the resulting solution showed a ν_{CO} band at 1921 cm^{-1}. Crystals of $[NEt_4]_3[Fe_5C(CO)_{13}(COMe)]$ suitable for X-ray diffraction were obtained by layering n-hexane (2 mL) and diisopropyl ether (40 mL) on the MeCN solution.

Characterization of $[NEt_4]_3[Fe_5C(CO)_{13}(COMe)]$:

IR (MeCN, 298K) ν_{CO}: 1988(w), 1920(vs), 1793(w) cm^{-1}

IR (Nujol, 298 K) ν_{CO}: 1933(s), 1905(s) cm^{-1}

4.5 Reaction of $[NEt_4]_4[Fe_6C(CO)_{15}]$ with EtI in the presence of Na_2CO_3: Synthesis of $[NEt_4]_3[Fe_5C(CO)_{13}(COEt)]$

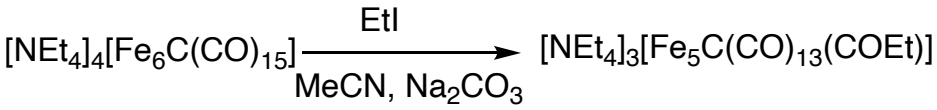

$[NEt_4]_4[Fe_6C(CO)_{15}]$ (0.37 g, 0.288 mmol) was solubilized in MeCN (20 mL) and then, Na_2CO_3 (6.08 mg, 0.057 mmol) was added. A solution of EtI (387 μL, 4.81 mmol) in MeCN (5 mL) was prepared, and added to the solution of the cluster in three portions (0.2 mL, 0.2 mL and 0.1 mL). At the end of the reaction, there was IR evidence of the presence in the solution of $[NEt_4]_2[Fe_6C(CO)_{16}]$ (ν_{CO} 1966 cm^{-1}) and $[NEt_4]_3[Fe_5C(CO)_{13}(COEt)]$ (ν_{CO} 1919 cm^{-1}).

The solvent was evaporated under vacuum and the solid was washed with H_2O (20 mL) and toluene (20 mL).

$[NEt_4]_2[Fe_6C(CO)_{16}]$ was removed from the solid residue with THF (70 mL), whereas the extraction in acetone (10 mL) contained a major amount of $[NEt_4]_2[Fe_6C(CO)_{16}]$ together with a minor product showing ν_{CO} at 1920 cm^{-1} which is supposed to be the product of interest with formula $[NEt_4]_3[Fe_5C(CO)_{13}(COEt)]$.

The residue was, then, extracted with MeCN (10 mL) and the resulting solution showed a ν_{CO} band at 1919 cm^{-1}which was attributable to a purported species $[NEt_4]_3[Fe_5C(CO)_{13}(COEt)]$.

Characterization of $[NEt_4]_3[Fe_5C(CO)_{13}(COEt)]$:

IR (MeCN, 298K) ν_{CO}: 1919cm^{-1}

4.6 Reaction of $[NEt_4]_4[Fe_6C(CO)_{15}]$ with EtI: Synthesis of $[NEt_4]_3[Fe_5C(CO)_{13}(COEt)]$ and $[NEt_4]_3[H_3O][Fe_6C(CO)_{14}(CO_3)]$

$$[NEt_4]_4[Fe_6C(CO)_{15}] \xrightarrow[MeCN]{EtI} [NEt_4]_3[Fe_5C(CO)_{13}(COEt)]$$

$[NEt_4]_4[Fe_6C(CO)_{15}]$ (0.37 g, 0.288 mmol) was solubilized in MeCN (20 mL). A solution of EtI (392 μL, 0.490 mmol) in MeCN (5 mL) was prepared, and added to the solution of the cluster in different portions (0.2 mL, 0.2 mL and 0.3 mL). At the end of the reaction, there was IR evidence of the presence in the solution of $[NEt_4]_2[Fe_6C(CO)_{16}]$ (ν_{CO} 1966 cm^{-1}) and $[NEt_4]_3[Fe_5C(CO)_{13}(COEt)]$ (ν_{CO} 1919 cm^{-1}).

The reaction products were precipitated adding a saturated solution of $[NEt_4]Br$ in H_2O to the MeCN solution.

The solid was recovered upon filtration, dried under vacuum and washed with H_2O (20 mL) and toluene (20 mL).

$[NEt_4]_2[Fe_6C(CO)_{16}]$ was removed from the solid residue with THF (70 mL). The residue was then extracted with acetone (20 mL) and the resulting solution showed a ν_{CO} band at 1917 cm^{-1} together with other two bands attributable to $[NEt_4]_2[Fe_5C(CO)_{14}]$ (ν_{CO} 1962 and 1947 cm^{-1}).

Crystals of $[NEt_4]_3[H_3O][Fe_6C(CO)_{14}(CO_3)]$ suitable for X-ray diffraction were obtained by layering n-hexane (80 mL) on the acetone solution.

The extraction in MeCN (10 mL) contained unreacted $[NEt_4]_4[Fe_6C(CO)_{15}]$ (ν_{CO} 1875 cm^{-1}), $[NEt_4]_2[Fe_5C(CO)_{14}]$ (ν_{CO} 1963 and 1950 cm^{-1}), and the purported $[NEt_4]_3[Fe_5C(CO)_{13}(COEt)]$ (ν_{CO} 1919 cm^{-1}), all characterized by IR spectroscopy.

Characterization of $[NEt_4]_3[H_3O][Fe_6C(CO)_{14}(CO_3)]$:

IR (acetone, 298 K) ν_{CO}: 2015 (w),1947(vs), 1785 (w) cm^{-1}

IR (Nujol, 298K) ν_{CO}: 1940 cm^{-1}

Characterization of $[NEt_4]_3[Fe_5C(CO)_{13}(COEt)]$:

IR (MeCN, 298K) ν_{CO}: 1919 cm^{-1}

4.7 Reaction of $[NEt_4]_4[Fe_6C(CO)_{15}]$ with $HBF_4 \cdot Et_2O$: Synthesis of $[NEt_4]_2[Fe_5C(CO)_{14}]$

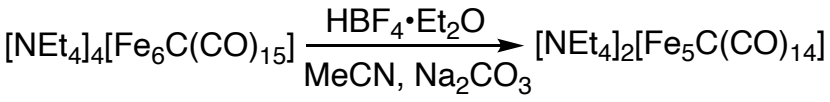

Reaction (a)

$[NEt_4]_4[Fe_6C(CO)_{15}]$ (0.20 g, 0.155 mmol) was solubilized in MeCN (15 mL) and then, Na_2CO_3 (16.4 mg, 0.155 mmol) was added. A solution of $HBF_4 \cdot Et_2O$ (40 μL, 0.311 mmol) in MeCN (2 mL) was prepared, and added to the solution of the cluster. At the end of the reaction, there was IR evidence of the presence in the solution of $[NEt_4]_2[Fe_5C(CO)_{14}]$ (ν_{CO} 1965 and 1949 cm^{-1}). The solvent was evaporated under vacuum and the solid was washed with H_2O (20 mL) and toluene (20 mL).

$[NEt_4]_2[Fe_5C(CO)_{14}]$ was extracted with THF (20 mL). Crystals of $[NEt_4]_2[Fe_5C(CO)_{14}]$ suitable for X-ray diffraction were obtained by layering n-hexane (80 mL) on the THF solution (20 mL).

Characterization of $[NEt_4]_2[Fe_5C(CO)_{14}]$:

IR (THF, 298K) ν_{CO}: 2026(w), 1962(vs), 1948(s), 1779(w) cm^{-1}

IR (Nujol, 298K) ν_{CO}: 1954(m), 1929(m) cm^{-1}

Reaction (b)

$[NEt_4]_4[Fe_6C(CO)_{15}]$ (0.25 g, 0.194 mmol) was solubilized in MeCN (15 mL) and then, Na_2CO_3 (20.5 mg, 0.194 mmol) was added. A solution of $HBF_4 \cdot Et_2O$ (50 μL, 0.388 mmol) in MeCN (2 mL) was prepared, and added to the solution of the cluster. At the end of the reaction, there was IR evidence of the presence in the solution of a mixture of products: $[NEt_4]_2[Fe_5C(CO)_{14}]$ (ν_{CO} 1965 and 1949 cm^{-1}), an unknown compounds showing ν_{CO} at 1915 cm^{-1}, and a small amount of unreacted $[NEt_4]_4[Fe_6C(CO)_{15}]$ (ν_{CO} 1872 cm^{-1}).

The solvent was evaporated under vacuum and the solid was washed with H_2O (20 mL) and toluene (20 mL).

$[NEt_4]_2[Fe_5C(CO)_{14}]$ was removed from the solid residue with THF (20 mL), whereas the extraction in acetone (5 mL) contained the same compound present in THF as well as an unknown compound (ν_{CO} 1913 cm^{-1}) and unreacted $[NEt_4]_4[Fe_6C(CO)_{15}]$ (ν_{CO} 1872 cm^{-1}).

$[NEt_4]_2[Fe_5C(CO)_{14}]$ (ν_{CO} 1965 and 1948 cm^{-1}) was extracted with MeCN (10 mL).

Characterization of the unknown compounds extracted with acetone:

IR (acetone, 298 K) ν_{CO}: 1913cm^{-1}

4.8 Reaction of $[NEt_4]_4[Fe_6C(CO)_{15}]$ with $[Cp_2Fe][PF_6]$

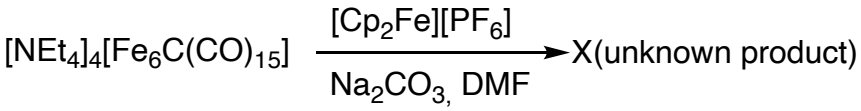

$[NEt_4]_4[Fe_6C(CO)_{15}]$ (0.35 g, 0.272 mmol) was solubilized in DMF (10 mL) and then, Na_2CO_3 (23 mg, 0.272 mmol) was added. A solution of $[Cp_2Fe][PF_6]$ (170 mg, 0.544 mmol) in DMF (2 mL) was prepared, and added (0.2 mL) to the cluster solution. At the end of the reaction, there was IR evidence of a mixture of products: $[NEt_4]_2[Fe_6C(CO)_{16}]$ (ν_{CO} 1965 cm^{-1}), an unknown product (ν_{CO} 1944 and 1915 cm^{-1}), and unreacted $[NEt_4]_4[Fe_6C(CO)_{15}]$ (ν_{CO} 1872 cm^{-1}).

The solution was precipitated with a saturated solution of $[NEt_4]$ in H_2O and then, the solid residue, was washed with H_2O (3 x 20 mL) to eliminate all the salts present in solution and, then, with toluene (20 mL).

$[NEt_4]_2[Fe_6C(CO)_{16}]$ was removed from the solid residue with THF (40 mL), whereas the extraction in acetone (5 mL) contained the same compound present in the previous extraction and an unknown product showing a ν_{CO} band at 1920 cm^{-1}.

The residue was then extracted with MeCN (10 mL) and the resulting solution showed a ν_{CO} band at 1875 cm^{-1}. Crystals of $[NEt_4]_4[Fe_6C(CO)_{15}]$ suitable for X-ray diffraction were obtained by layering n-hexane (2 mL) and diisopropyl ether (40 mL) on the MeCN solution.

Characterization of $[NEt_4]_4[Fe_6C(CO)_{15}]$:

IR (MeCN, 293 K) ν_{CO}: 1875(vs), 1732(m) cm^{-1}

4.9 Reaction of $[NEt_4]_4[Fe_6C(CO)_{15}]$ with S_8

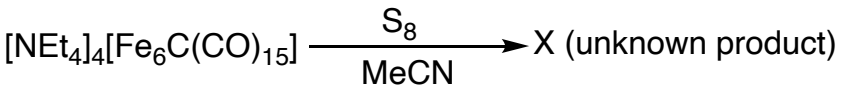

$[NEt_4]_4[Fe_6C(CO)_{15}]$ (0.35 g, 0.272 mmol) was solubilized in MeCN (20 mL) and then, S_8 was added (9 mg, 0.280 mmol). At the end of the reaction, there was IR evidence of the presence in the solution of $[NEt_4]_2[Fe_5C(CO)_{14}]$ (ν_{CO} 1965 and 1949 cm^{-1}) and an unknown product (ν_{CO} 1920 cm^{-1}).

The solvent was evaporated under vacuum and the solid was washed with H_2O (20 mL) and toluene (20 mL).

$[NEt_4]_2[Fe_6C(CO)_{16}]$ was removed from the solid residue with THF (20 mL), whereas the extraction in acetone (10 mL) contained $[NEt_4]_2[Fe_5C(CO)_{14}]$ (ν_{CO} 1963 and 1946 cm^{-1}).

The extraction in MeCN (10 mL) contained a mixture of unknown products (ν_{CO} 1948, 1919 and 1907 cm^{-1}), and unreacted $[NEt_4]_4[Fe_6C(CO)_{15}]$ (ν_{CO} 1875 cm^{-1}).

Characterization of the unknown products extracted with CH_3CN:

IR (MeCN, 298K) ν_{CO}: 1948(m), 1919(s), 1907(vs) cm^{-1}

4.10 Reaction of $[NEt_4]_4[Fe_6C(CO)_{15}]$ with PhSH: Synthesis of $[NEt_4]_3[Fe_6C(CO)_{14}(SPh)]$

Reaction (a):

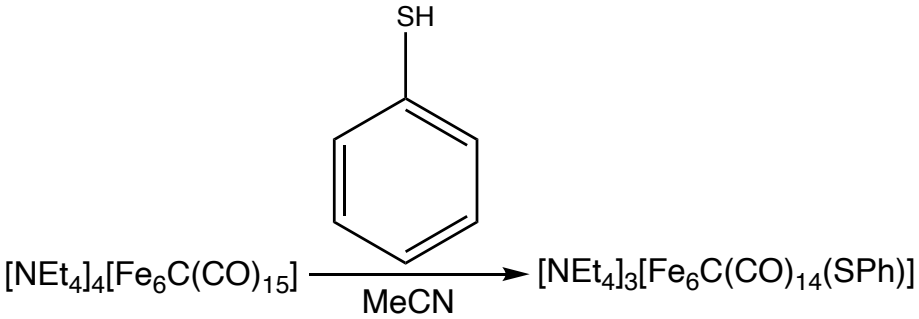

$[NEt_4]_4[Fe_6C(CO)_{15}]$ (0.35 g, 0.272 mmol) was solubilized in MeCN (30 mL). A solution of PhSH (28 μL, 0.235 mmol) in MeCN (5 mL) was prepared and added dropwise in different portions (0.8 mL in total) to the cluster solution. At the end of the reaction, there was IR

evidence of the presence in the solution of $[NEt_4]_2[Fe_5C(CO)_{14}]$ (ν_{CO} 1965 and 1949 cm^{-1}) and an unknown product (ν_{CO} 1920 cm^{-1}).

The solvent was evaporated under vacuum and the solid was washed with H_2O (20 mL) and toluene (20 mL).

$[NEt_4]_2[Fe_6C(CO)_{16}]$ was removed from the solid residue with THF (20 mL); whereas the extraction in acetone (10 mL) contained mainly $[NEt_4]_2[Fe_5C(CO)_{14}]$ (ν_{CO} 1964 and 1946 cm^{-1}) and in smaller amount a product attributable to a purported $[NEt_4]_3[Fe_6C(CO)_{14}(SPh)]$ species (ν_{CO} 1912 cm^{-1}).

From the extraction in acetone, crystals of $[NEt_4]_3[H_3O][Fe_6C(CO)_{14}(CO_3)]$ suitable for X-ray diffraction were obtained by layering n-hexane (50 mL) on the acetone solution.

The residue was, then, extracted with MeCN (10 mL) and the resulting solution showed a ν_{CO} at 1875 cm^{-1}. Crystals of $[NEt_4]_4[Fe_6C(CO)_{15}]$ suitable for X-ray diffraction were obtained by layering n-hexane (2 mL) and diisopropyl ether (40 mL) on the MeCN.

Characterization of $[NEt_4]_3[Fe_6C(CO)_{14}(SPh)]$:

IR (acetone , 298K) ν_{CO}: 1912(vs) cm^{-1}

IR (MeCN, 298 K) ν_{CO}: 1989(w), 1913(vs), 1794 (w)cm^{-1}

Reaction (b):

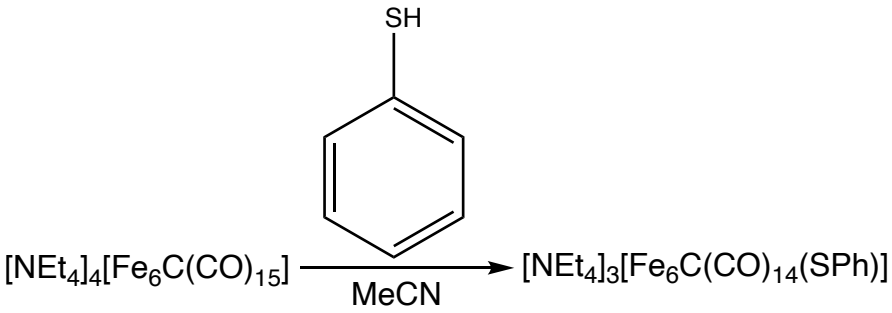

$[NEt_4]_4[Fe_6C(CO)_{15}]$ (0.36 g, 0.280 mmol) was solubilized in MeCN (30 mL). A solution of PhSH (29 μL, 0.272 mmol) in MeCN (5 mL) was prepared and added dropwise in different portions (1.4 mL in total) to the cluster solution. At the end of the reaction, there was IR evidence of the presence in the solution of $[NEt_4]_2[Fe_5C(CO)_{14}]$ (ν_{CO} 1967 and 1949 cm^{-1}) and the new species $[NEt_4]_3[Fe_6C(CO)_{14}(SPh)]$ (ν_{CO} 1913 cm^{-1}).

The solvent was evaporated under vacuum and the solid was washed with H_2O (20 mL) and toluene (20 mL).

$[NEt_4]_2[Fe_6C(CO)_{16}]$ was removed from the solid residue with THF (10 mL), whereas the extraction in acetone (10 mL) contained a major amount of $[NEt_4]_2[Fe_5C(CO)_{14}]$ (ν_{CO} 1965 and 1945 cm^{-1}) and a minor amount attributable to $[NEt_4]_3[Fe_6C(CO)_{14}(SPh)]$ (ν_{CO} 1912 cm^{-1}).
The extraction in MeCN (5 mL) contained $[NEt_4]_3[Fe_6C(CO)_{14}(SPh)]$ (ν_{CO} 1912 cm^{-1}) as major product, as well as a minor amount of $[Fe_5C(CO)_{14}]^{2-}$ (ν_{CO} 1966 and 1947 cm^{-1}).
Crystals of $[NEt_4]_3[Fe_6C(CO)_{14}(SPh)]$ suitable for X-ray diffraction were obtained by layering n-hexane (2 mL) and diisopropyl ether (40 mL) on the MeCN solution.

Characterization of $[NEt_4]_3[Fe_6C(CO)_{14}(SPh)]$:
IR (acetone , 298K) ν_{CO}: 1912 cm^{-1}
IR (MeCN, 298 K) ν_{CO}: 1989(w), 1913(vs), 1794 (w) cm^{-1}

4.11 Reaction of $[NEt_4]_4[Fe_6C(CO)_{15}]$ with S_2Cl_2

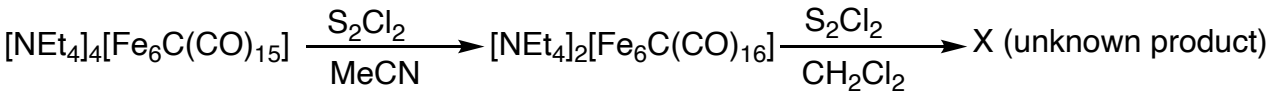

$[NEt_4]_4[Fe_6C(CO)_{15}]$ (0.36 g, 0.280 mmol) was solubilized in MeCN (30 mL). A solution of S_2Cl_2 (45 μL, 0.560 mmol) in MeCN (5 mL) was prepared and all the solution was added dropwise to the cluster solution. At the end of the reaction, there was IR evidence of the presence in the solution of $[NEt_4]_2[Fe_6C(CO)_{16}]$ (ν_{CO} 1965 cm^{-1}).
The solvent was evaporated under vacuum and the solid was dissolved into CH_2Cl_2 (30 mL).
The oxidant S_2Cl_2 was added directly to the cluster solution in two portions (2 ×7 μL), over a period of 2 days.
At the end of the reaction, there was IR evidence of the presence in the solution of unknown products showing ν_{CO} at 2003 and 2040 cm^{-1}.
Unknown compounds showing ν_{CO} bands at high wavenumbers were removed in THF (10 mL); whereas the extraction with acetone (10 mL) contained a major amount of an unknown compound showing a ν_{CO} band at 2007 cm^{-1} and a minor amount of an unknown compound showing a ν_{CO} band at 2029 cm^{-1}.

Characterization of the unknown compounds:

IR (THF, 298K) ν_{CO}: 2027(w), 2006(s), 1988(w) cm^{-1}

IR (acetone, 298 K) ν_{CO}: 2031(w), 2006(s), 1983(w) cm^{-1}

5. References

[1] F. A. Cotton, *Q. Rev. Chem. Soc.* **1966**, 389-401.

[2] I. Ciabatti, *"Dalla scoperta del nichel tetracarbonile alla sintesi di nanocondensatori molecolari ad elevata nuclearità"*. Rendiconti Accademia Nazionale delle Scienze detta dei XL, Memorie di Scienze Chimiche Naturali **2014**, 45-57.

[3] D. M. P. Mingos, *Pure & Appl. Chem.* **1991**, *63*, 807-812.

[4] J. W. Lauher, *J. Am. Chem. Soc.* **1978**, *100*, 5305-5315.

[5] S. Zacchini, *Eur. J. Inorg. Chem.* **2011**, 4126-4129.

[6] W. Hieber, F. Leutert, *Die Naturwissenschaften*, **1931**, *19,* 360-361.

[7] P. Chini, *Inorg. Chim. Acta*, **1968**, *2*, 31-51.

[8] E. H. Braye, L. F. Dahl, W. Hübel, D. L. Wampler, *J. Am. Chem. Soc.* **1962**, *84*, 4633-4639.

[9] A. Sirigu, M. Bianchi, E. Benedetti, *Chem. Commun.* **1969**, 596-597.

[10] A. Reinholdt, J. Bendix*, Chem. Rev.* **2022**, *122*, 830-902.

[11] S. Takemoto, H. Matsuzaka, *Coord. Chem. Rev.* **2012**, *256*, 574-588.

[12] C. Cesari, J.-H. Shon, S. Zacchini, L. A. Berben, *Chem. Soc. Rev.* **2021**, *50*, 9503-9539.

[13] J. H. Davis, M. A. Beno, J. M. Williams, J. Zimmie, M. Tachikawa, E. L. Muetterties, *Proc. Nat. Acad. Sci.* **1981**, *78*, 668-671.

[14] J. S. Bradley, *Adv. Organomet. Chem*. **1983**, *22*, 1-58.

[15] M. Tachikawa, E. L. Muetterties, *Prog. Inorg. Chem.* **1981**, *28*, 203-238.

[16] M. Tachikawa, R. L. Geerts, E. L. Muetterties, *J. Organomet. Chem.* **1981**, *213*, 11-24.

[17] P. M. Maitlis, V. Zanotti, *Chem. Commun.* **2009**, 1619-1634.

[18] I. T. Moraru, L. M. Martínez-Prieto, Y. Coppet, B. Chaudret, L. Cusinato, I. del Rosal, R. Poteau, *Nanoscale* **2021**, *13*, 6902-6915.

[19] Q.-Y. Liu, C. Shang, Z.-P. Liu, *J. Am. Chem. Soc.* **2021**, *143*, 11109-11120.

[20] J. Ohata, A. Teramoto, H. Fijita, S. Takemoto, H. Matsuzaka, *J. Am. Chem. Soc.* **2021**, *143*, 16105-16112.

[21] P. Braunstein, L. A. Oro, P. R. Raithby (Eds.), Metal Clusters in Chemistry, Wiley-VCH, Weinheim, **1999**.

[22] G. Schmid (Ed.), Clusters and Colloids, Wiley-VCH, Weinheim, **1994**.

[23] B. F. G. Johnson, J. Lewis, S. W. Sankey, K. Wong, M. McPartlin, W. J. H. Nelson, *J. Organomet. Chem.* **1980**, *191*, C3-C7.

[24] M. R. Churchill, J. Wormald, J. Knight, M. J. Mays, *J. Am. Chem. Soc.* **1971**, *93*, 3073-3074.

[25] C. Femoni, M. C. Iapalucci, F. Kaswalder, G. Longoni, S. Zacchini, *Coord. Chem. Rev.* **2006**, *250*, 1580-1604.

[26] K. M. Lancaster, M. Roemelt, P. Ettenhuber, Y. Hu, M. W. Ribbe, F. Neese, U. Bergmann, S. DeBeer, *Science* **2011**, *334*, 974-977.

[27] J. A. Rees, R. Bjornsson, J. Schlesier, D. Sippel, O. Einsle, S. DeBeer, *Angew. Chem. Int. Ed.* **2015**, *54*, 13249-13252.

[28] T. M. Buscagan, K. A. Perez, A. O. Maggiolo, D. C. Rees, T. Spatzal, *Angew. Chem. Int. Ed.* **2021**, *60*, 5704-5707.

[29] C. Joseph, C. R. Cobb, M. J. Rose, *Angew. Chem. Int. Ed.* **2021**, *60*, 3433-3437.

[30] C. Joseph, J. P. Shupp, C. R. Cobb, M. J. Rose, *Catalysts* **2020**, *10*, 1317.

[31] C. Joseph, S. Kuppuswamy, V. M. Lynch, M. J. Rose, *Inorg. Chem.* **2018**, *57*, 20-23.

[32] L. Liu, T. J. Woods, T. B. Rauchfuss, *Eur. J. Inorg. Chem*. **2020**, 3460-3465.

[33] L. Liu, T. B. Rauchfuss, T. J. Woods, *Inorg. Chem*. **2019**, *58*, 8271-8274.

[34] S. Pattanayak, L. A. Berben, *ChemElectroChem* **2021**, *8*, 2488-2494.

[35] A. Taheri, L. A. Berben, *Inorg. Chem.* **2016**, *55*, 378-385.

[36] A. D. Nguyen, M. Diego Rail, M. Shanmugam, J. C. Fettinger, L. A. Berben, *Inorg. Chem.* **2013**, *52*, 12847-12854.

[37] A. V. Virovets, E. Peresypkina, M. Scheer, *Chem. Rev.* **2021**, *121*, 14485-14554.

[38] G. Longoni, A. Ceriotti, R. Della Pergola, M. Manassero, M. Perego, G. Piro, M. Sansoni, *Philos. Trans. R. Soc. A* **1982**, *308*, 47-57.

[39] J. S. Bradley, G. B. Ansell, M. E. Leonowicz, E. W. Hill, *J. Am. Chem. Soc.* **1981**, *103*, 4968-4970.

[40] A. Gourdon, Y. Jeannin, *J. Organomet. Chem.* **1985**, *290*, 199-211.

[41] M. Bortoluzzi, I. Ciabatti, C. Cesari, C. Femoni, M. C. Iapalucci, S. Zacchini, *Eur. J. Inorg. Chem.* **2017**, 3135-3143.